

https://dspace.org/

A study of the parameters affecting the design of vertical spindle mills

De Wet Kruger, John Ivor

2015-03-05
http://hdl.handle.net/10539/17158

Downloaded from a DSpace repository. https://dspace.org/

UNIVERSITY OF THE WITWATERSRAND

SCHOOL OF MECHANICAL ENGINEERING

A STUDY OF THE PARAMETERS AFFECTING THE DESIGN OF VERTICAL SPINDLE MILLS

by

JOHN IVOR DE WET KRÜGER

A dissertation submitted to the Faculty of Engineering, University of the Witwatersrand, Johannesburg, for the degree of Master of Science in Engineering.

Johannesburg
1977

DECLARATION

I, John Ivor de Wet Krüger, hereby declare that this dissertation is my own work and has not been submitted as a dissertation for the degree of Master of Science in Engineering to any other University.

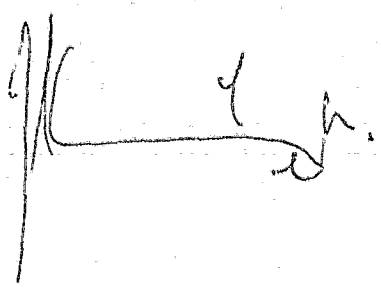

ABSTRACT

This dissertation is concerned with a study of the operating parameters of vertical spindle mills. The initial objective of the investigation was the study of the aerodynamics of air/coal mixtures within a coal mill with the object of optimising the design for future plants. This necessarily broadened out into aninvestigation of sampling procedures, coal properties and other inter-related mill parameters, in the course of which both model and field tests on a Loesche LM 18 pressure type roller mill and a Lopulco LM 14/3P pressure type roller mill (installed at Arnot and Camden Power Stations, Eastern Transvaal, respectively) were conducted.

On the experimental side, a 1/6th scale perspex model of a Lopulco LM 13/3P mill was constructed and mounted in a water circuit. Flow patterns were observed by means of pitot searches, stringers and polystyrene beads being introduced as 'feed' material. These tests were supplemented by tests on a 1/8th scale slice model using water, with coloured soap bubbles as the tracer element. Various geometries were inserted into these models and the flow patterns photographed. Further laboratory work was conducted on a fluidized bed rig using both air and water as fluidizing media. Familiarity was thus gained with the mechanism of fluid beds and the suitability of various equations to describe the flows was thereby established.

The model studies showed what had been expected, namely, that the flow patterns within typical mills was poor.

The Coanda (jet attachment) effect was particularly noticeable and was in fact recognised as a poor design feature on the Arnot mill due to the high wear rates it caused within that mill. The need for louvre configuration and body geometry design changes was also evident. Temperature and voidage measurements confirmed the existence of a region of high air heat transfer above the throat as well as high voidage in the main body of the mill. The fluid bed tests generally correlated well with existing data, and a bed fluctuation frequency - bed mass relationship was found which does not appear to have been described previously.

The Arnot tests were a follow-up to the model tests and provided a verification of some of the effects noted in the models. These tests were run concurrently with the power station commissioning work. Data for the Camden milling tests was taken from an extensive series of mill tests conducted by ICAL and ESCOM engineering personnel, the object being to optimise the mill operating parameters.

A comprehensive literature survey was made, and visits to various research institutions in England and Germany were also undertaken to study various aspects of the mill design problem.

ACKNOWLEDGEMENTS

This project was initiated and sponsored by International Combustion Africa Limited (ICAL) to whom the author wishes to record his grateful thanks; in particular he wishes to thank the following for their help and encouragement: Mr. A.L. Dunlop, Mr. W. Guest, Mr. D. Kirkman, Mr. J. Hill and members of the Operating and Test Department; Professors B.W. Skews and E.A. Bunt for their interest and support and for helpful comments during the drafting of this dissertation; Mr. T. O'D. Duggan and members of the Mechanical Engineering laboratory for all their advice and hard work during the model testing stages; and his family for their continued encouragement and support.

TABLE OF CONTENTS

	page
DECLARATION	(i)
ABSTRACT	(ii)
ACKNOWLEDGEMENTS	(iv)
TABLE OF CONTENTS	(v)
FIGURES	(xi)
TABLES	(xvii)
DEFINITIONS	(xviii)
LIST OF SYMBOLS	(xix)
CHAPTER 1: FOREWORD	1
1.0 Introduction	1
1.1 Object of the Study	1
1.2 Organisation of the Study	3
CHAPTER 2: THE PROBLEM OF SELECTING A TYPE OF MILL	5
2.0 Introduction	5
2.1 Size Reduction	5
2.2 Material Properties	6
2.3 Mill Categories	7
2.3.1 Tube Mill	8
2.3.1.1 Wet and Dry Grinding	9
2.3.2 Vertical Spindle Mills	11
2.3.2.1 Bowl Mill	12
2.3.2.2 Centrifugal Roll Mill	12
2.3.2.3 Ball Ring Roller Mill	14
2.3.2.4 Roll Ring Mill	14
2.3.2.5 Table and Roller Mill	14
2.3.3 Hammer and Beater Mills	14
2.3.3.1 Hammer Mill	17
2.3.3.2 Beater Mill	17

page

CHAPTER 2 (Cont'd)

2.4 Ball and Roller Mill Comparisons 17
2.5 Various Configurations of Milling Plant Layout 17
2.5.1 Open Circuit Pressure System . . . 21
2.5.2 Open Circuit Suction System . . . 21
2.5.3 Closed Circuit Milling 23

CHAPTER 3: SURVEY ON MILL RESEARCH FINDINGS AND ASSOCIATED PARAMETERS 27

3.0 Introduction 27
3.1 Milling and Milling Tests 27
3.2 Wear in Mills 35
3.3 Combustion 41
3.4 Particle Size Distribution Representation . 42
3.5 Pulverized Fuel Measurement 49
3.5.1 Sampling Procedures and Flow Measurement 49
3.6 Size Reduction 53
3.6.1 Kick's, Rittinger's and Bond's Laws . 54
3.6.2 Further Relationships 55

CHAPTER 4: DESIGN AND THEORETICAL ANALYSES OF MILL OPERATING PRINCIPLES 57

4.0 Introduction 57
4.1 Mill Selection 57
4.1.1 Coal Throughput 58
4.1.2 Product Size 59
4.1.3 Air Requirements 60
4.1.4 Grinding Media 61
4.1.5 Mill Power Requirements 62
4.1.6 Air Flow and Temperature Regulation 63
4.1.7 Throat Width 65

page

CHAPTER 4 (Cont'd)

4.2 Mill Operation and Operating Parameters . 70

4.2.1 P.A. differential 70
4.2.2 Mill differential 71
4.2.3 Air/Fuel Ratio 72
4.2.4 Separator Settings 72
4.2.5 Roll Pressure 74
4.2.6 Dam Ring 75
4.2.7 Reject Adjustment 77

4.3 Conclusion 78

CHAPTER 5: MILL MODEL TESTS 79

5.0 Scope of Tests 79
5.1 Physical Factors 79
5.2 Flow Visualisation 80
5.3 Model Design 82
5.4 3-Dimensional Mill Model Tests 83
5.5 Results of 3-Dimensional Model Tests . . 89

5.5.1 Flow Visualisation using Water and Beads 89
5.5.2 Pitot Traverse 91

5.6 Slice Model Tests 97
5.7 Jet Attachment above the Throat 99
5.8 Results of Slice Model Tests 101
5.9 Conclusions 110

CHAPTER 6: FLUIDIZED BED TESTS 111

6.0 Early Development of Fluidization Techniques 111
6.1 Application to Grinding 112
6.2 Mechanism of Operation of Fluid Bed . . . 114
6.3 Particulate and Aggregative Flow 117
6.4 Dense and Dilute Phases 117
6.5 Fixed Beds 118

page

CHAPTER 6 (Cont'd)

6.6 Minimum Fluidization 119
6.7 Expanded Bed 124
6.7.1 Solid-Liquid Systems 124
6.7.2 Solid-Air Systems 126
6.8 Experimental Apparatus 126
6.8.1 Air Fluidization 126
6.8.2 Water Fluidization 127
6.9 Bed Preparation 127
6.10 Sample Preparation 130
6.11 General Procedure 131
6.12 Results 131
6.12.1 Particle Size 131
6.12.2 Fixed Bed 133
6.12.3 Slugging 138
6.12.4 Minimum Fluidization 142
6.12.5 Expanded Bed (Liquid-solid) . . 143
6.12.6 Expanded Bed (Solid-Air) . . . 149
6.13 Conclusions 149

CHAPTER 7: INDUSTRIAL TESTS 154
7.0 Introduction 154
7.1 Arnot Tests 154
7.1.1 Introduction 154
7.1.2 Principle of Operation 155
7.1.3 Testing Programme 155
7.1.4 Throat Design 156
7.1.4.1 Throat Pressure Drop . . 157
7.1.4.2 Experimental Approach . . 159
7.1.5 Comment on Full Scale Throat Tests 166
7.1.6 Mill Operational Temperature Gradient 168

page

CHAPTER 7 (Cont'd)

7.1.7 Mill Operational Voidage . . . 170
7.1.8 Establishing Recirculating Load . 170
7.1.9 Separator Velocity Traverse . . 173
7.1.10 Separator Performance 175
7.1.11 Roll Speed 178
7.1.12 Coal Characteristics in Relation to Wear 178

7.2 Camden Tests 180
7.2.1 Principle of Operation of Lopulco LM 14/3P Mill 182
7.2.2 Sampling 183
7.2.2.1 Introduction 183
7.2.2.2 Rotating Arm Sampler . . 184
7.2.2.3 Sliding Arm Sampler . . 184
7.2.3 Coal Labelling 186
7.2.4 Interpreting Mill Results . . . 189

7.3 Conclusions from Industrial Tests . . . 191

CHAPTER 8: DISCUSSION OF DESIGN CONSIDERATIONS . . 193

8.0 Introduction 193
8.1 Future Design Considerations 193
8.1.1 Mill Drive 196
8.1.2 Mill Size 198
8.1.3 Materials 200
8.1.4 Conclusion 200

CHAPTER 9: SUGGESTIONS FOR FUTURE WORK 202

CHAPTER 10: CONCLUSIONS 203

10.1 Introduction 203
10.2 Mill Model Tests 203
10.3 Fluidized Bed Tests 204
10.4 Industrial Tests 204

		page
APPENDIX A:	REFERENCES	206
APPENDIX B:	ASSOCIATED LABORATORY AND SAMPLING EQUIPMENT	222
B1	Hardgrove machine	223
B2	Abrasive Index	223
B3	Rotap sieving machine	225
B4	Grindability Index	225
B5	Isokinetic sampler	226
B6	I.C.L. probe	229
APPENDIX C:	DRAWING OF ORIFICE PLATE AND CALIBRATION REFERENCE CURVES	230
APPENDIX D:	COMPARATIVE MILL PERFORMANCE CURVES . .	234
APPENDIX E:	CAMDEN MILL OPERATING PARAMETERS PLOTTED USING UNIFORMITY COEFFICIENT AND AVERAGE PARTICLE SIZE	239

TABLE OF FIGURES

page

CHAPTER 2

2.1 Continuous gravity-discharge multiple compartment tube mill 10
2.2 Conical ball mill 10
2.3 Autogenous mill 10
2.4 Bowl mill -- deep bowl 13
2.5 Bowl mill - shallow bowl 13
2.6 Centrifugal roll mill 15
2.7 Ball ring roller mill 15
2.8 Roll ring mill 16
2.9 Suction roller mill 16
2.10 Hammer mill 18
2.11 Beater mill 18
2.12 Throughput vs milling power 19
2.13 Throughput vs cost/t 19
2.14 Throughput vs machine mass 20
2.15 Throughput vs relative purchase price . 20
2.16 Open circuit pressure system 22
2.17 Open circuit suction system 22
2.18 Closed circuit system with vertical spindle mill 24
2.19 Closed circuit system with ball mill . . 24
2.20 Closed circuit system with air heater . 26

CHAPTER 3

3.1 Correlation of grindability indices . . 29
3.2 Voidage measurements on a ring roll mill 31
3.3 Separator characteristics 33
3.4 Typical classifier test layout 33
3.5 Wear rate tests 37
3.6 Mill output vs roller and table wear . . 37
3.7 Wear rate in Yancey Geer and Price test . 39

page

CHAPTER 3 (Cont'd)

3.8 Mill and laboratory wear rates 39

3.9 Alpha quartz in coal vs wear rate for LM 1.6 mill 40

3.10 Particle mass histogram 44

3.11 Particle mass cumulative curve 44

3.12 Typical p.f. sample distribution . . . 46

3.13 Relationship between pitot-static differential pressure and density ratio of dust -air mixture 50

3.14 Annular venturi 52

CHAPTER 4

4.1 Typical starting torque on load . . . 63

4.2 Air/coal control curve 64

4.3 P.A. diff - mill diff curves 71

4.4 Air/fuel ratio vs throughput curve . . 72

4.5 Roll pressure conditions 75

4.6 Roll and table wear 76

4.7 Roll ridge pattern 76

4.8 Coal wave ahead of roll 77

CHAPTER 5

5.1 Mill model layout 85

5.2 Feed bin and model 87

5.3 General view of model and discharge arrangement 87

5.4 Mill top 88

5.5 View into mill from top showing throat . 88

5.6 Mill body 88

5.7 Cone inserts 88

5.8 Roll insert 88

5.9 Polystyrene beads - flow pattern between rolls 90

5.10 Polystyrene beads - flow pattern around roll 90

page

CHAPTER 5 (Cont'd)

5.11 Reverse flow indicated by stringers . . 90
5.12 Pitot traverse of model - Test 1 . . . 92
5.13 Pitot traverse of model - Test 2 . . . 93
5.14 Dead space above table 96
5.15 Separator blade wear 96
5.16 Test cone inserts 96
5.17 The slice model mounted on the hydraulic bench 98
5.18 - 5.21 Jet attachment data 100
5.22 - 5.39 Slice model visualisation results . . . 104 to 109

CHAPTER 6

6.1 Typical representation of the fluidization curve 116
6.2 Values of ε_{mf} in relation to d 121
6.3 Voidage function and shape factor correlation 121
6.4 Comparison of correlations for predicting onset of fluidization 123
6.5 The generalized correlation of Wilhelm and Kwauk 123
6.6 Slope values from gas and liquid-fluidized data in relation to particle size . . . 126
6.7 Air fluidization 128
6.8 Water fluidization 128
6.9 The experimental rig (water-solid) . . 129
6.10 Pressure drop nomenclature 134
6.11 Constant 2 C vs air velocity 135
6.12 Bed height vs bed mass 136
6.13 Pressure drop through a packed restrained column 137
6.14 Pressure drop-velocity curves for an air fluidized bed 139
6.15 Frequency vs velocity ratio for a particular bed height 140
6.16 Peak frequency vs bed height 141

page

CHAPTER 6 (Cont'd)

6.17 Voidage vs velocity ratio with theoretical curves superimposed - solid-liquid . . . 144

6.18 $(1-\varepsilon)/\varepsilon^3$ vs Re for solid-liquid expansion 145

6.19 Voidage vs Reynolds Number for solid-liquid expansion 148

6.20 Voidage of an expanding bed - solid-air . 150

6.21 $(1-\varepsilon)/\varepsilon^3$ vs Re for solid-air expansion . 151

6.22 Bed expansion curve with no slugging . . 152

CHAPTER 7

7.1 LM 18 mill undergoing works testing . . 157

7.2 Mill diff vs P.A. diff for various louvre configurations 161

7.3 Vertical square inlet edged louvre . . . 162

7.4 The K factor for various shapes tested . 162

7.5 Cone sections fitted above throat . . . 162

7.6 Original louvre throat configuration . . 164

7.7 Original armour ring 164

7.8 Modified armour ring 164

7.9 Bypass cone 164

7.10 Bypass throat 167

7.11 The 65° mild steel armour ring in position 167

7.12 Experimentally measured temperature profile in Loesche LM 18D mill 169

7.13 M.P.S.mill temperature profile 169

7.14 Voidage profiles in a Loesche LM 18D mill 171

7.15 Clean air traverse of Loesche separator . 174

7.16 Flow pattern in vanes 176

7.17 Separator characteristics for Loesche LM 18D mill 177

7.18 Fineness variation vs outlet sleeve position 179

7.19 Effect of roll pressure variation on mill power and roll r/min 179

7.20 Cost correlation from South African Power Stations 181

7.21 Correlation of Hardgrove and Abrasive Indices 181

page

CHAPTER 7 (Cont'd)

7.22 Lopulco mill assembled in works . . . 182
7.23 Rotating arm sampler 185
7.24 Sliding arm sampler 185
7.25 Sampler test results 187
7.26 Time vs number of counts for irradiated Camden coal 188

CHAPTER 8

8.1 Large cement raw meal mill - Loesche LM 32/4 195
8.2 Gearbox for Loesche LM 32/4 mill . . . 195
8.3 New drive arrangement for a roller mill . 198
8.4 Proposed air by-pass system 200

APPENDIX B

B.1 Hardgrove machine 224
B.2 Isokinetic sampler 227
B.3 Typical conditions in a vertical coal pipe 228
B.4 I.C.L. sampler probe 229

APPENDIX C

C.1 Orifice plate and flange for model water circuit 231
C.2 Calibration curve for orifice plate . . 232
C.3 Model feed bin reference curve . . . 233

APPENDIX D

D.1 Mill capacity curves vs Hardgrove Index for various types of mill 235
D.2 Design curve for a roller mill . . . 236

APPENDIX E

E.1 Average particle size vs air/fuel ratio . 242
E.2 Uniformity coefficient n vs air/fuel ratio at constant load 243

page

APPENDIX E (Cont'd)

E.3 Uniformity coefficient n vs throat velocity 244

E.4 Average particle size vs throat velocity 244

E.5 Uniformity coefficient n vs separator r/min at constant load 245

E.6 Average particle size vs separator r/min at constant load 245

E.7 Uniformity coefficient n vs mill throughput 246

E.8 Average particle size vs mill throughput 246

E.9 Uniformity coefficient n vs spring tenaion 247

E.10 Average particle size vs spring tension 247

E.11 Separator dust loading vs average particle size 248

LIST OF TABLES

page

CHAPTER 2

2.1 Size reduction categories 6
2.2 Mohs' scale of hardness 7

CHAPTER 6

6.1 Free fall velocity data 132
6.2 Packed bed voidages 133
6.3 Minimum fluidization velocity data . . 142
6.4 Expanded bed results 143
6.5 Experimental results of Richardson and Zaki equation 146
6.6 Experimental slope and particle size comparison 147
6.7 Experimental results from Figure 6.21 . 149

CHAPTER 7

7.1 Clean air pressure drop 158

DEFINITIONS

A/F	-	Air/Fuel (ratio)
BCURA	-	British Coal Utilisation Research Association
CEGB	-	Central Electricity Generating Board
ESCOM	-	Electricity Supply Commission
FD	-	Forced Draught
ICAL	-	International Combustion Africa Limited
ICL	-	International Combustion Limited
LM 16/3	-	LM stands for Lopulco Mill, 16 denotes the table size and 3 the number of rolls
Mill Diff	-	Mill 'differential' pressure (normally mill inlet pressure less mill outlet pressure)
% minus mesh	-	% of material mass passing through a specified mesh size opening
PA	-	Primary Air
PA diff	-	Primary Air differential pressure
Pf	-	Pulverised fuel
Seal Air	-	High pressure air supplied to mechanical moving parts in the mill pressurised zone

LIST OF SYMBOLS

Roman	Symbol	Units	Description
	A	L^2	Area
	A_g	L	Geometric mean
	b	-	Constant
	C	L^{-3}	Number concentration of particles
		-	Constant (Chapter 6)
	C_c	-	Area ratio
	C_D	-	Drag coefficient
	D_t	L	Tube diameter
	D(x)	M	Mass passing through sieve mesh
	d	L	Particle diameter
	e	-	Exponential function
	F	-	Function of
	F_D	MLT^{-2}	Drag force
	F_n	-	Fluidization number
	f	L	Feed size
		-	Friction factor
	G	$MT^{-1}L^{-2}$	Mass velocity
	H	T^{-1}	Peak frequency
	H_i	M	Hardgrove Index
	h	L	Throat distance from re-attachment surface
	K	-	Size modulus constant
		-	Throat factor (Chapter 7)
	K_o	MT^{-1}	Initial grinding rate for reference size X_o

Symbol	Units	Description
K_1 to K_{11}	-	Constants
L	L	Bed height
	L	Length size of flow (Chapter 3)
l	L	Re-attachment length
M	-	Distribution modulus constant
$\dot{M}$	MT^{-1}	Flow rate
m	-	Constant
$\dot{m}$	MT^{-1}	Wear rate
N	-	Constant
n	-	Constant
$\mathcal{N}$	-	Uniformity coefficient
P	$ML^{-1}T^{-2}$	Pressure
ΔP	$ML^{-1}T^{-2}$	Pressure drop
R	-	Reynolds number ratio
Re	-	Reynolds number
R(x)	M	Mass residue on sieve mesh
R_L	-	Recirculating load
r	L	Particle radius
	L	Flow path radius (Chapter 7)
S	L^2	Surface area
s	$ML^{-1}T^{-2}$	Stress
T	MT^{-1}	Mass throughput (Chapter 7)
t	T	Time
	L	Throat width
v	LT^{-1}	Velocity
W	L^2T^{-2}	Work/mass
W_i	$M^{1/2}L^2T^{-2}$	Work index

Symbol	Units	Description
X_o	L	Reference size
x	L	Particle size (usually defined by the mesh size)
x_o	L	Absolute size

Greek	Symbol	Units	Description
	α	-	Constant
		(deg)	Angle
	γ	-	Constant
	ε	-	Voidage
	μ	$ML^{-1}T^{-1}$	Dynamic viscosity
	ρ	ML^{-3}	Mass density
	ϕ_s	-	Shape factor
	σ	-	Standard deviation

Subscripts

A, B	-	differentiates between two conditions
C	-	vena contracta
f	-	fluid
m	-	mean
o	-	superficial (velocity)
s	-	solid

Subscripts

T	-	throat
t	-	terminal
mb	-	mill body
mf	-	minimum fluidization
mi	-	mill inlet
PA	-	primary air
ε	-	voidage
1, 2	-	refers to two conditions $1 > 2$ for particle size

CHAPTER 1

FOREWORD

1.0 INTRODUCTION

The comminution of coal and industrial minerals has in the past been regarded as more of an art than a science for the reason that there have been no fixed boundaries within which parameters could be inter-related with any degree of certainty. Due to the very nature of the raw material - rock, sand, clay, etc - and the variability of its composition and chemistry, it has been difficult and often risky attaching too much significance to previous experience or laboratory data. The process is in itself of such a destructive nature that it almost defies the placing on it of physical and analytical constraints. However, when it is realised that an enormous energy drain is taking place during this crude transition called comminution, it is worth investigating whether or not this process can be better understood. This brings one into the realms of kinetics, statistics, probability theory and breakage functions, as well as a host of relationships involving material properties, fluidized beds, pneumatic conveying and heat transfer. A quick scan through the literature will verify that the above subjects have been investigated thoroughly, although not always conclusively, during the past thirty to forty years.

1.1 OBJECT OF THE STUDY

When this project was embarked upon, the intention was to study the aerodynamics of a particular roller mill. However, due to the complex parameters and phenomena involved in such an investigation, it soon became apparent that a broader basis of investigation should be undertaken to try and link up the inter-related phenomena. The work embarked upon therefore includes experimental work on

fluidized beds, a water model of a roller mill and a slice model of the same mill with flow visualisation, and roller-mill tests were also conducted in situ at a power station. Furthermore, the author also made full use of such full scale test data as was readily available to illustrate certain relevant aspects.

The aims may thus be stated as:

(i) *The gaining of an insight into the flow of an* air-solid mixture within a roller mill with a view to optimisation of flow conditions.
(ii) Presentation of test data relating to the mill tests in such a way that trends are simplified and may be easily inter-related.
(iii) Presentation of design considerations arising out of performance data.

Since the author's professional association was with Lopulco and Loesche mills (both of which are of the vertical spindle type), the scope of investigation has therefore centred on the characteristics of these mills, (although the same basic principles are applied to most mills), as described briefly in Chapter 2. Supplementary information on wear rates and coal properties was obtained from a survey of various power stations in South Africa undertaken with the object of relating various mill types and coals with respect to wear rate and maintenace and their direct effect-cost relationships.

1.2 ORGANIZATION OF THE STUDY

The dissertation is presented as a series of chapters on general design considerations and various experiments relating to the overall study.

Chapter 2 outlines the classification of materials with regard to type of breakage required, and includes brief descriptions of some of the principles of operation of industrially available mills. Typical layouts of tube and vertical spindle mills are presented here.

Chapter 3 includes a literature survey on various aspects of milling and its associated parameters. Relevant research and development projects are also described briefly.

Chapter 4 contains a discussion on various design and selection criteria as well as explanatory notes on operational parameters.

Chapter 5 describes tests on a model Lopulco mill.

Chapter 6 describes air and water fluidization studies undertaken.

Chapter 7 contains the results of full scale tests on the Loesche Mill at Arnot Power Station Power Station and an analysis of test data on sampling from Camden Power Station.

Design considerations, as applicable in future concepts, are discussed in Chapter 8.

Chapter 9 puts forward a number of research avenues suggested by this study which could profitably be followed up.

Chapter 10 summarises the main conclusions arising from the experimental work described in Chapters 5, 6 and 7.

Typical laboratory standard tests as well as mill parameters using the uniformity coefficient.
and average particle size are presented in the Appendix, and a detailed list of references is also given.

CHAPTER 2

THE PROBLEM OF SELECTING A TYPE OF MILL

2.0 INTRODUCTION

Industry today is dependent on a multitude of commodities, raw and refined, which have undergone a size reduction or a grinding, comminution or degradation process at some stage of manufacture. For example, cement, flour and face powder have entirely different end uses but are all subjected to mechanical impact of one kind or another to produce the final powdery substance. One lump of 25 mm coal reduced to minus 100 mesh (150μm) is broken into three or more million individual pieces with the resultant expenditure of a large amount of energy. The material has therefore undergone a permanent physical change due to one of the above size reduction methods.

In power stations fired by pulverised coal, lumps of coal are ground to a powder and blown into the furnace for combustion purposes. In this form, combustion takes place more efficiently, and enables high heat releases to be relied upon when designing a furnace.

2.1 SIZE REDUCTION

The categories of size reduction can be loosely grouped as shown in the following table.

TABLE 2.1: Size Reduction Categories

Crushing	approximately 3 mm.
Very Coarse Grinding	a milled product of 3 mm down.
Coarse Grinding	10 mesh down.
Medium Fine Grinding	95 per cent minus 100 mesh.
Fine Grinding	95 per cent minus 200 mesh.
Very Fine Grinding	99 per cent minus 300 mesh.
Superfine Grinding	below 325 mesh and particularly to the 5 to 10 µm range.

The categories investigated in this study are Medium Fine to Very Fine Grinding.

2.2 MATERIAL PROPERTIES

The energy required to break a rock or lump will normally reflect the hardness or toughness of the material. At the same time, the wear and abrasion imparted by this hard material will impose physical restraints on the type of grinding media to be used. Various Indices are in use to differentiate to some degree between these physical differences, these being the Hardgrove Index, the Abrasive Index, and the Mohs' Hardness (Table 2.2), to mention only a few. The Hardgrove and Abrasive Index tests are briefly described in the Appendix.

TABLE 2.2: Mohs' Scale of Hardness (non-linear)

Hardness No	Represented by
1	Talc or graphite
2	Gypsum
3	Calcite
4	Fluorspar
5	Apatite
6	Felspar
7	Quartz
8	Topaz
9	Sapphire
10	Diamond

2.3 MILL CATEGORIES

The grinding process results from two main categories of mill, namely:

(i) tumbling mills
(ii) vertical spindle, beater and hammer mills.

Type (i) mills are used where Mohs' Hardness usually exceeds 5, although of course this type can be used at a lower hardness as well.

Type (ii) mills are used almost exclusively below a hardness of 5 on the Mohs' Scale, due to the very high wear rates that are experienced at higher hardnesses. In addition, grinding can take place in a wet or dry environment. By the very nature of the construction of the various types of mill, the tumbling type is the only type suited to wet grinding.

2.3.1 Tube Mill

As the name implies, a mill consists of a horizontally rotating tube in which the material to be ground is tumbled with a ball, rod or oversize feed (autogenous grinding) charge. Abrasive materials - whether drv or wet - are nearly always ground by this method since the wear of liners and ball or rod charge is not such a handicap on performance - for instance, the balls are added with the feed at pre-determined intervals of time, and the liners are made thick enough to last for a reasonable maintenance interval. Of course, there are instances where liners have to be replaced every 40 - 50 days for grinding quartz rock, as occurs on the gold mines, but this degree of wear on any other type of mill would result in maintenance shut-downs after shorter intervals of time.

Depending on the fineness of the grind required, one or more compartments are incorporated in the shell, as seen in the mill illustrated in Figure 2.1.

Material throughput is achieved bv either a load gradient within the mill whereby the material is forced from feed end to discharge end due to the discharge opening being larger, and therefore lower, than the feed trunnion, or by having lifters, or a peripheral discharge at the discharge end, the latter being used extensively on wet grinding installations.

Air sweeping can also be used in dry grinding to evacuate the fines and in this respect the system conforms to a conventional closed or open milling circuit. Such circuits will be discussed in Section 2.5.

A variation of the tube mill is the conical mill (Figure 2.2) which, by virtue of the centrifugal action decreasing with diameter, sizes the charge within the mill; this results in more efficient grinding, since the smaller ball charge grinds the finer material within the mill. (The feed enters at the smaller cone end).

For feed material that is both abrasive and of a wide size distribution, it is sometimes advantageous to let the rock grind itself ("autogenous" grinding). Such a mill is shown in Figure 2.3. A feature of these mills is the large diameter to length ratio necessary to ensure high impact of rock upon rock. The feed normally contains rocks of 300 mm and larger to ensure efficient grinding.

2.3.1.1 Wet and Dry Grinding

Both wet and dry grinding systems are in extensive use, the main parameter being the type of end use for which the powder or ground material is destined. For example, in wet grinding a flotation process follows the grinding event, and a slurry is pumped through cyclones to separate oversize particles for further grinding. There is no dust nuisance, and the powder is in an easily manageable form which can be piped away for storage in the open.

Very often a dry powder will present "wettability" problems if moisture is added after grinding. In addition, where intimate mixing and dissolving of solids is required, wet grinding is definitely preferred. Against this is the increased power absorption due to the mass of pulp in the mill and the higher power requirements for hydraulic transportation. A wet mill should be run as continuously as possible due to the time required to stabilise grinding conditions on re-start.

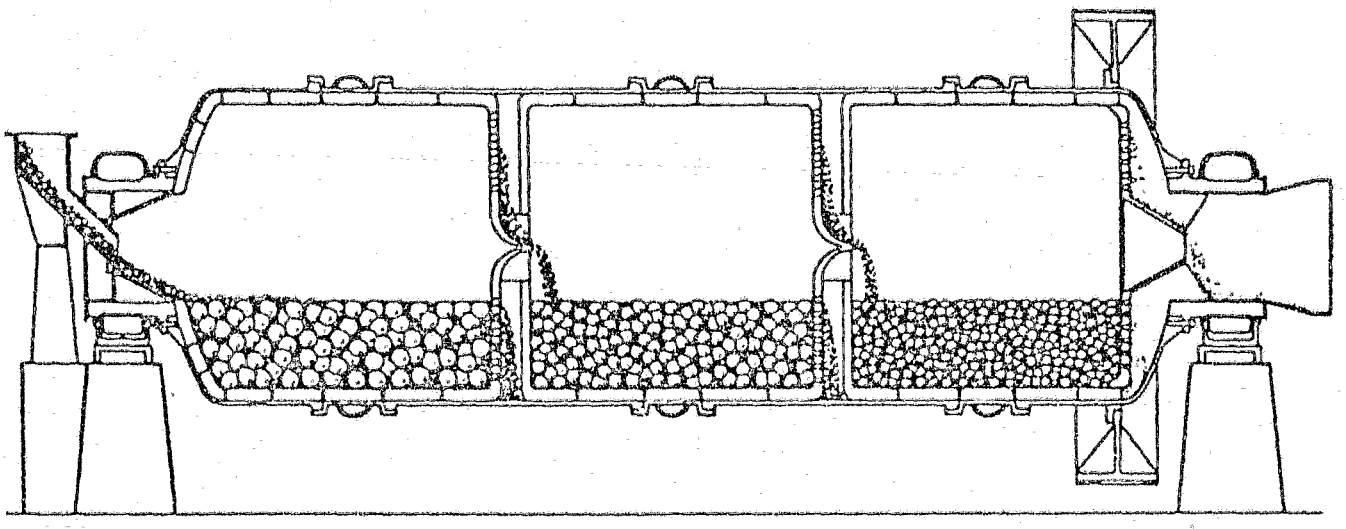

FIGURE 2.1: Continuous gravity-discharge multiple compartment tube mill (from M27)

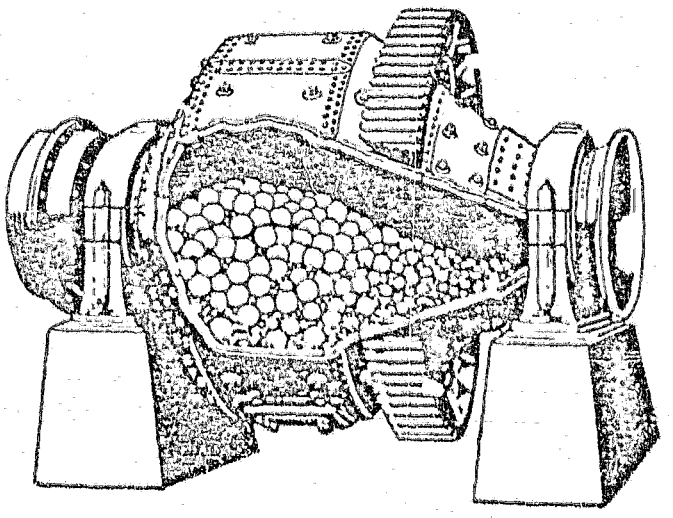

FIGURE 2.2: Conical ball mill (from M27)

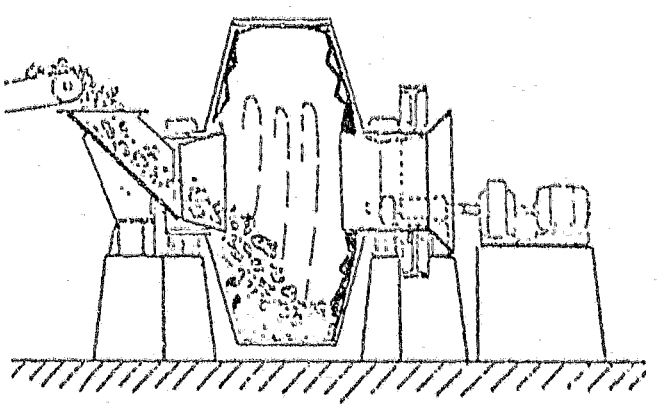

FIGURE 2.3: Autogenous mill (from M27)

Dry grinding is used where the final product has to be dry. Material can also be dried concurrent with the grinding operation by sweeping the mill with hot air or other gases. However, this introduces the need for cyclones, ducting and dust collection equipment which adds to the overall plant capital cost. If the grinding operation is intermittent, the dry grinding system will give a more consistently sized product due to the quick stabilising features and ease of start up and shut down.

The main parameters affecting the tube mill performance are mill speed, ball or rod charge, mill diameter and length. Secondary factors are air or water flow, feed size and trunnion size (which dictates the level to which the mill can be filled).

2.3.2 Vertical Spindle Mills

These mills have either a horizontally rotating table driven by a horizontal input, vertical output reduction gearbox, or rotating rolls running on a stationary grinding ring. Due to its design and mechanical features, this type of mill is suitable for grinding softer materials such as coal, clays and phosphates. Either a pressure or suction evacuating system is used, the former necessitating the supply of sealing air to mechanical moving parts such as bearings and shafts. A general advantage which the vertical spindle mill enjoys over a tube type mill is that power consumption per tonne is nearly half that of the ball or rod mill (dry grinding) and the grinding action is more easily controlled - for example, the roll grinding pressure is easily adjusted on

load with mills using hydraulic loading to control grinding pressure, and the control response is far quicker due to the swept volume advantage of the vertical spindle mill, and its method of air entrainment. A saving in floor space is also achieved over the tube mill as well as quieter operation.

2.3.2.1 Bowl Mill (Figures 2.4 and 2.5)

This is similar in air flow principle to other vertical spindle mills, the grinding action being accomplished by spring loaded rolls running on the sides of a rotating bow[illegible]ole. Due to centrifugal action, the material is th[illegible]own under the rolls, and in this respect the height and slope of the bowl are important for efficient grinding. This mill is normally operated under suction. An internal classification circuit returns oversize material for further grinding.

2.3.2.2. Centrifugal Roll Mill (Figure 2.6)

The central spindle positions three, four, five or six roller assemblies in the vertical hanging position, as shown. When the spindle is rotated, the centrifugal action causes the rolls to act as pendulums bearing against the outer hardened ring. The base of the spindle carries ploughs which scoop up the material from the base and throw it under the rolls where it is ground and swept up to a whizzer separator, or static classifier, as shown. Care must be taken to ensure continuous feed, otherwise possible damage can occur from the metal to metal contact of roll and ring, although the initial adjustment leaves a gap between rolls and ring. This mill is particularly well suited to grinding sticky materials.

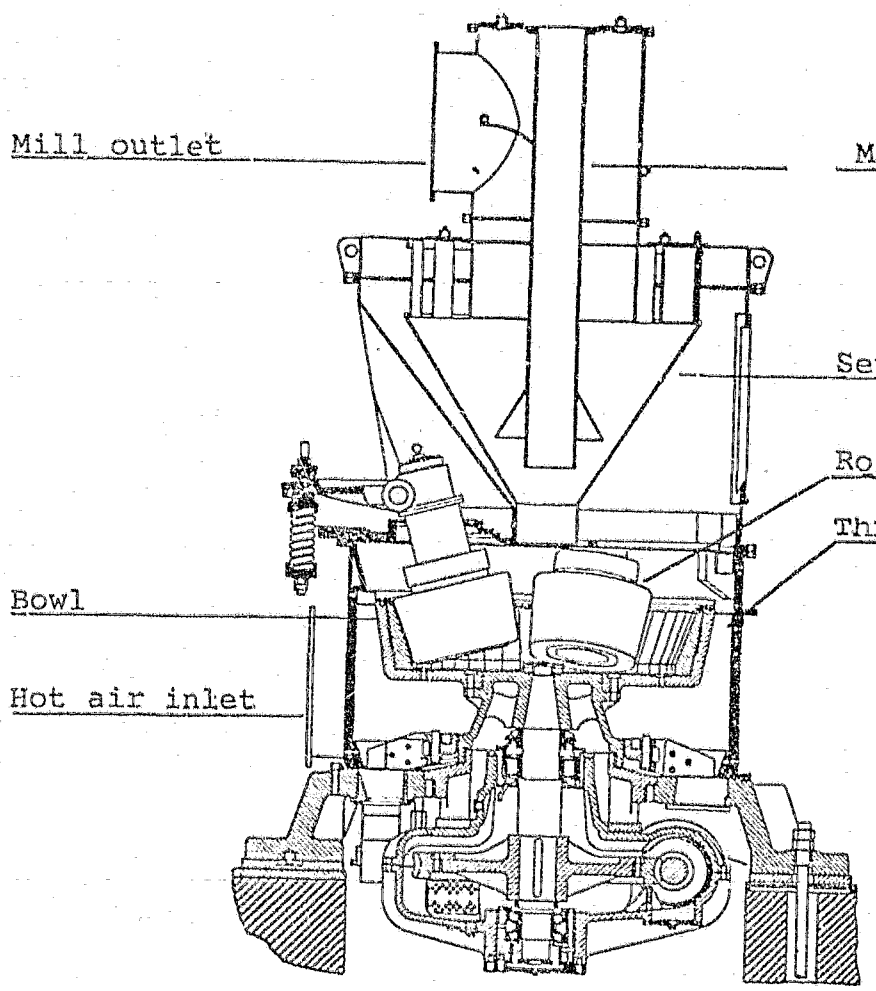

FIGURE 2.4:
Bowl mill - deep bowl

(from M33)

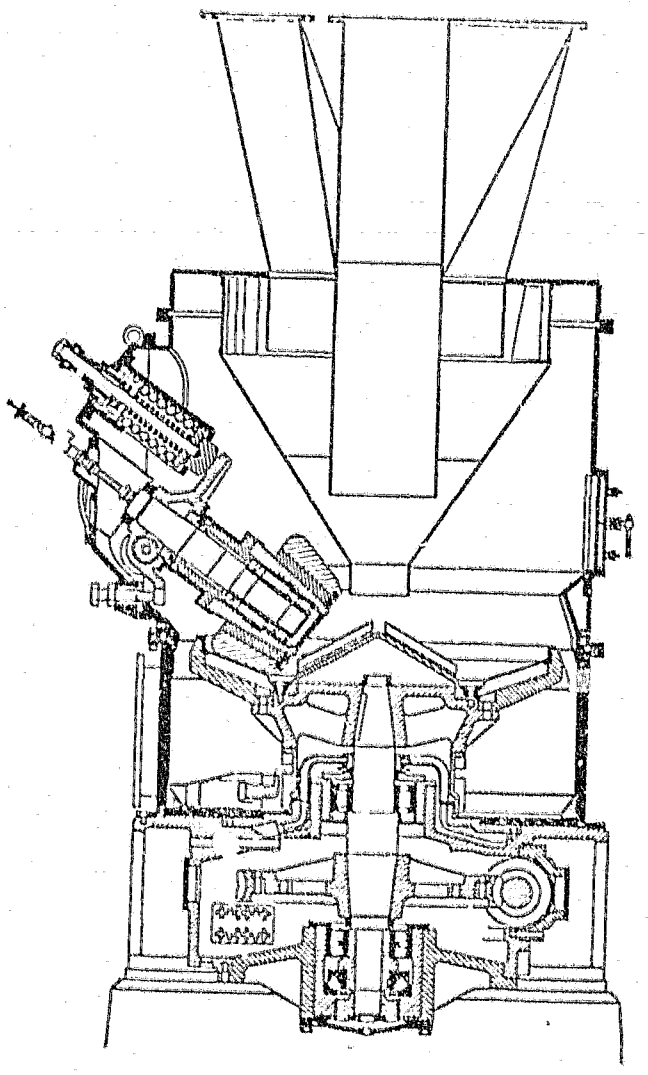

FIGURE 2.5:
Bowl mill - shallow bowl

(from M33)

2.3.2.3 Ball Ring Roller Mill (Figure 2.7)

This mill is unique in its mode of operation. The lower ring rotates on a yoke whilst the upper ring is stationary and pneumatically loaded. Hollow cast balls grind the material whilst revolving in the track, and air entrains the material, moving it to the separator. As the balls wear, replacement balls, equal in size to the remaining worn balls, are introduced into the track. Compared to similarly rated vertical spindle mills of other types, this mill is lower in overall height, but larger in diameter.

2.3.2.4 Roll Ring Mill (Figure 2.8)

This further variation of the ball ring roller mill has tyres running in a rotating lower track with a loaded upper frame supporting the tyres.

2.3.2.5 Table and Roller Mill (Figure 2.9)

Here a table driven by a right angle drive gearbox rotates in a horizontal plane with two, three or four rolls running under tension on the table. The ground material is throv off the table by centrifugal action into the annular space, from whence it is conveyed to the internal separator.

'Tramp' material collects in boxes at each side of the mill for manual removal.

2.3.3 Hammer and Beater Mills

When the coal is soft these mills can be used. In fact they are extensively used in power stations on the Continent with throughputs ranging up to 30 t/h and more. Comminution is by high speed mechanical impact.

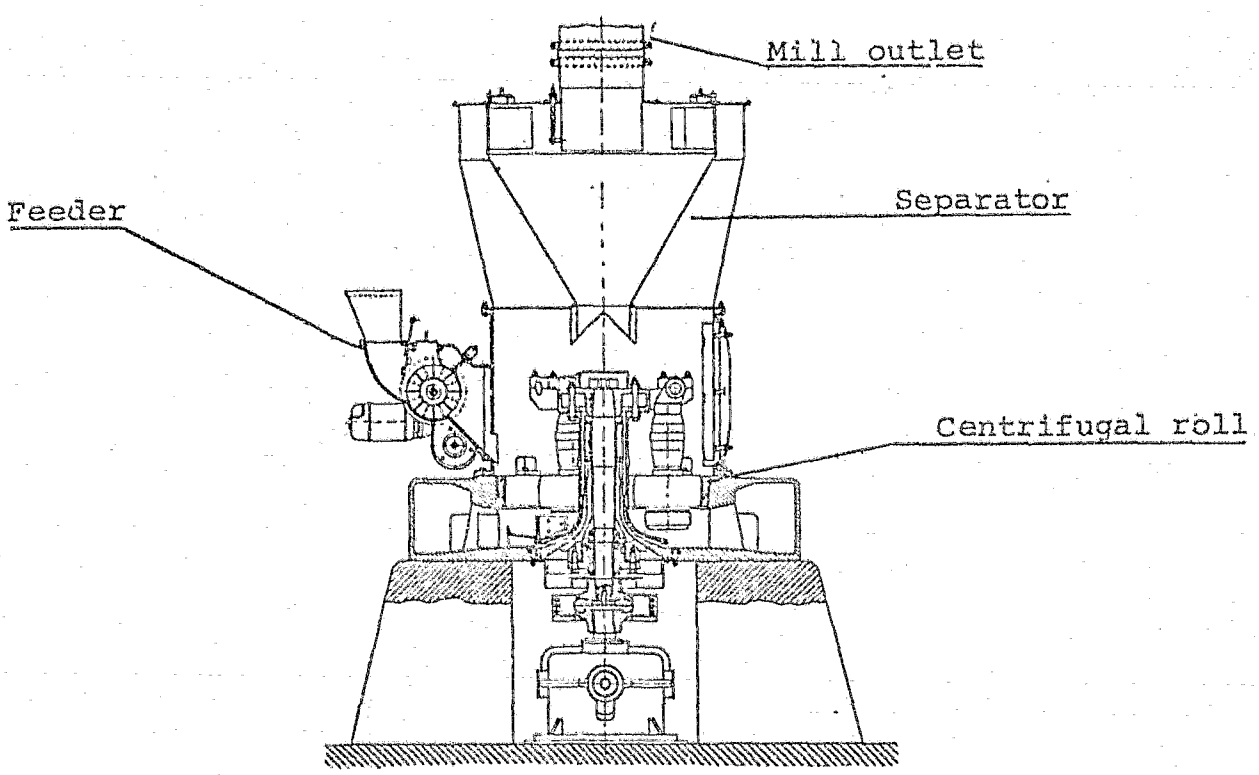

FIGURE 2.6: Centrifugal roll mill (from M33)

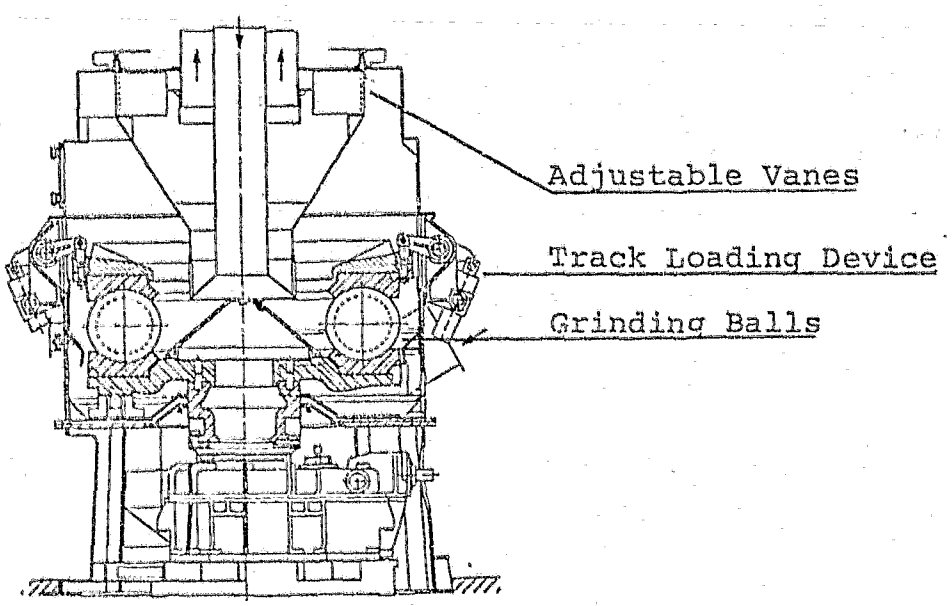

FIGURE 2.7: Ball ring roller mill (from M9)

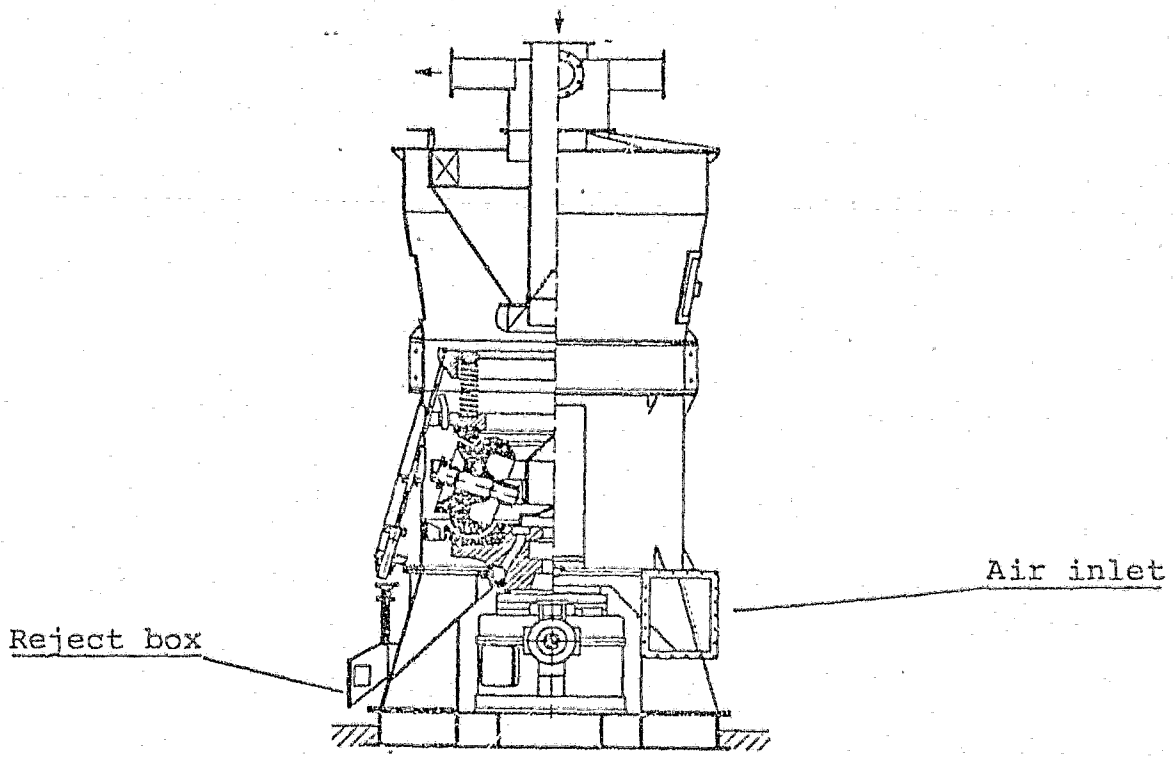

FIGURE 2.8: Roll ring mill (from M9)

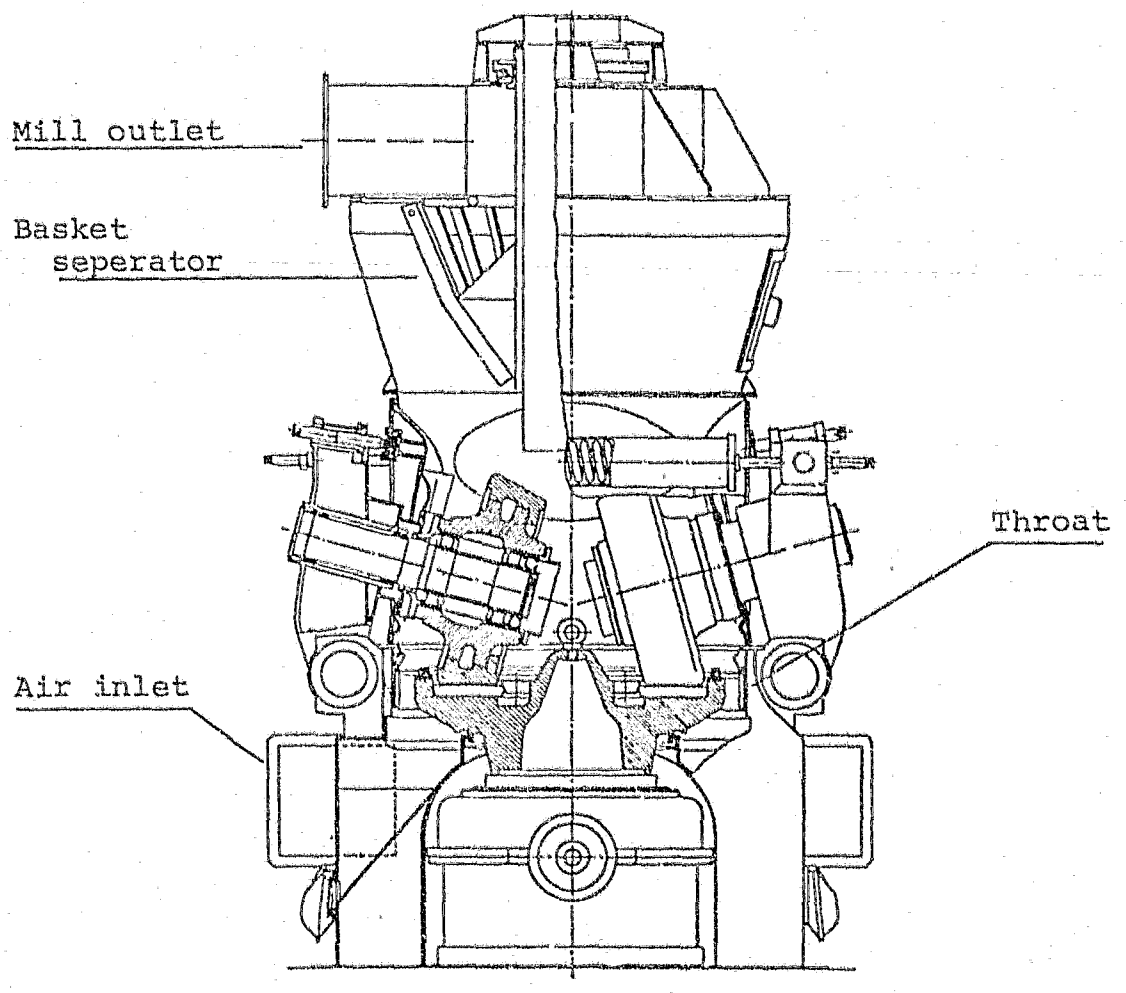

FIGURE 2.9: Suction roller mill (from M34)

2.3.3.1 Hammer Mill (Figure 2.10)

The rotating hammer heads provide effective comminution by impact and friction. Circumferential velocities of 4270 m/min are not uncommon. An internal classification circuit can be incorporated as shown.

2.3.3.2 Beater Mill (Figure 2.11)

This is essentially a paddle bladed fan also using impact for comminution, but generating a velocity head due to the fan action. Therefore, unlike the hammer mill which requires an external fan, the beater mill depends for its operation on the fan laws and is especially suitable for mill drying with hot flue gases and working against high static heads.

2.4 BALL AND ROLLER MILL COMPARISONS

These curves show power consumption, milling costs, mill mass, and purchase price comparisons for a ball mill and a roller mill. Clearly the roller mill is favoured by these comparisons for grinding comparable minerals (Figures 2.12, 2.13, 2.14 and 2.15).

2.5 VARIOUS CONFIGURATIONS OF MILLING PLANT LAYOUT

The type of mill selected will influence the milling circuit configuration, and a number of systems have been used to fire pulverised fuel into furnaces or kilns. In the following sections each one will be briefly described.

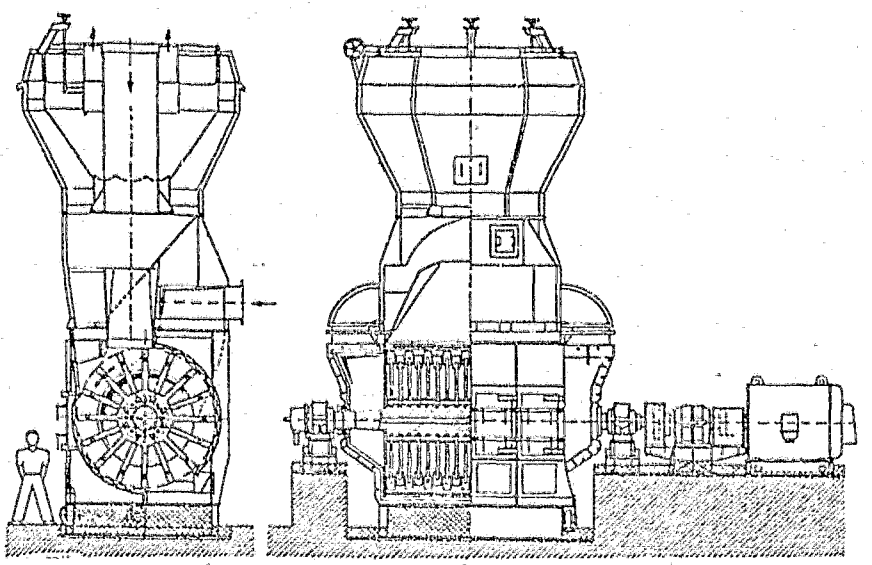

FIGURE 2.10: Hammer Mill (from M9)

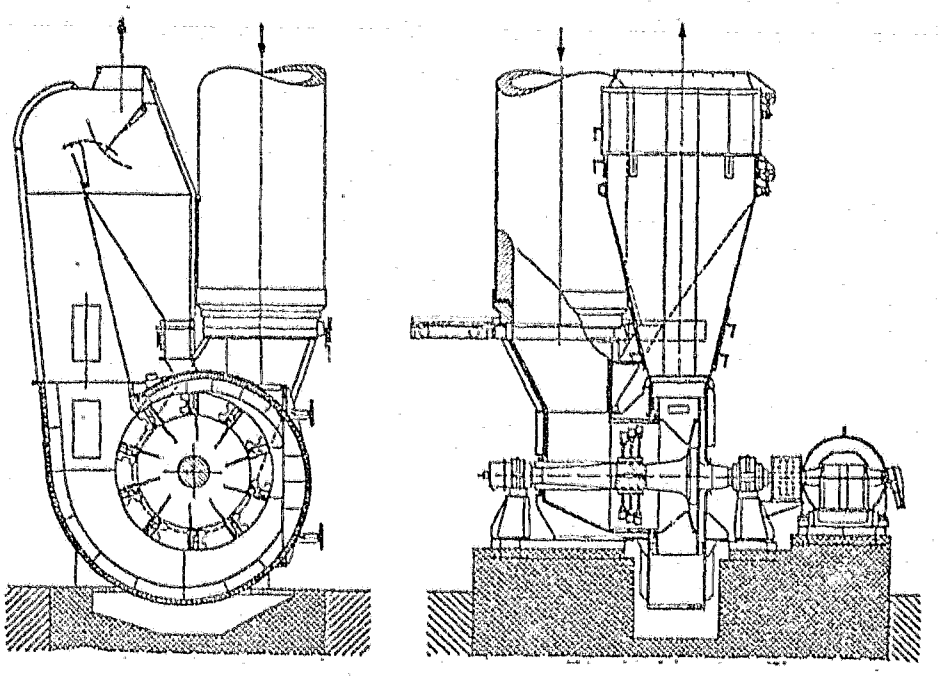

FIGURE 2.11: Beater mill (from M9)

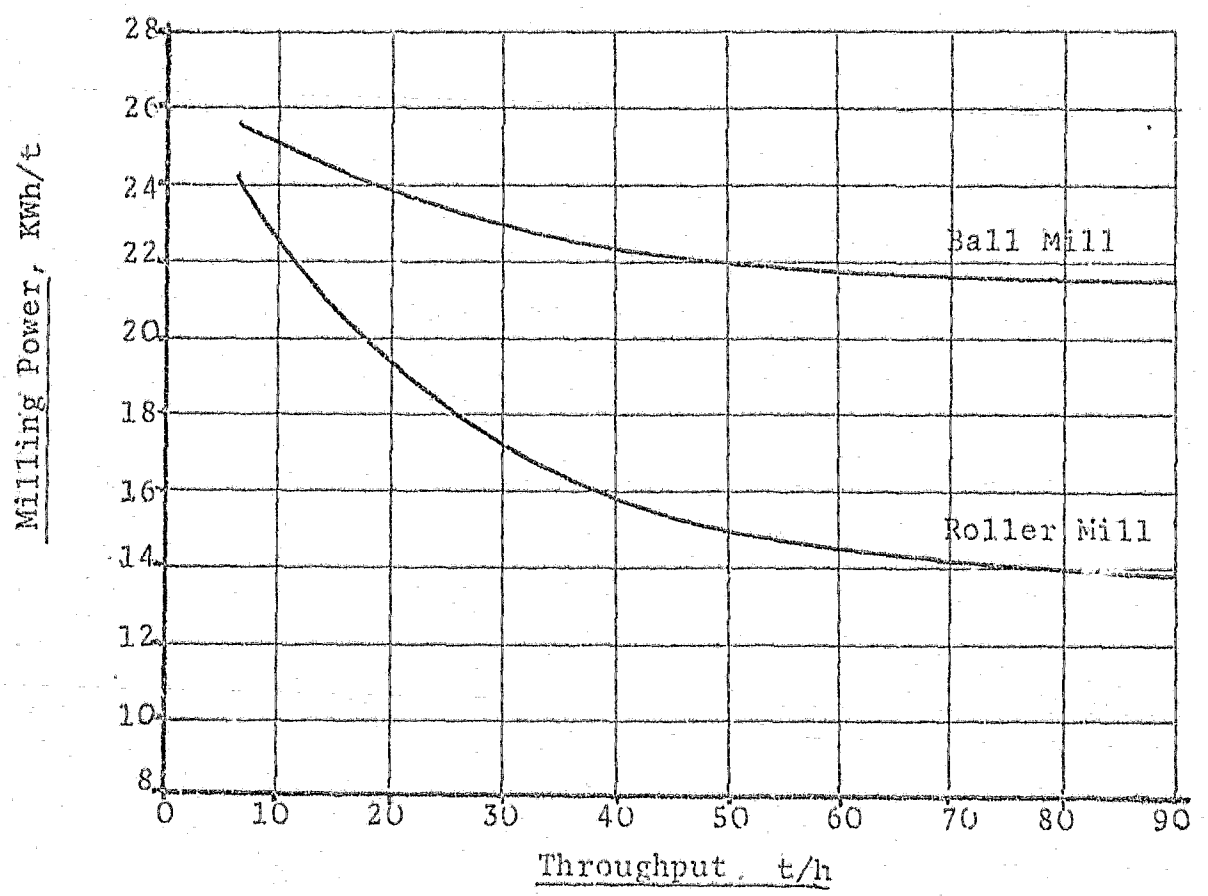

FIGURE 2.12 Throughput vs milling power (from M35)

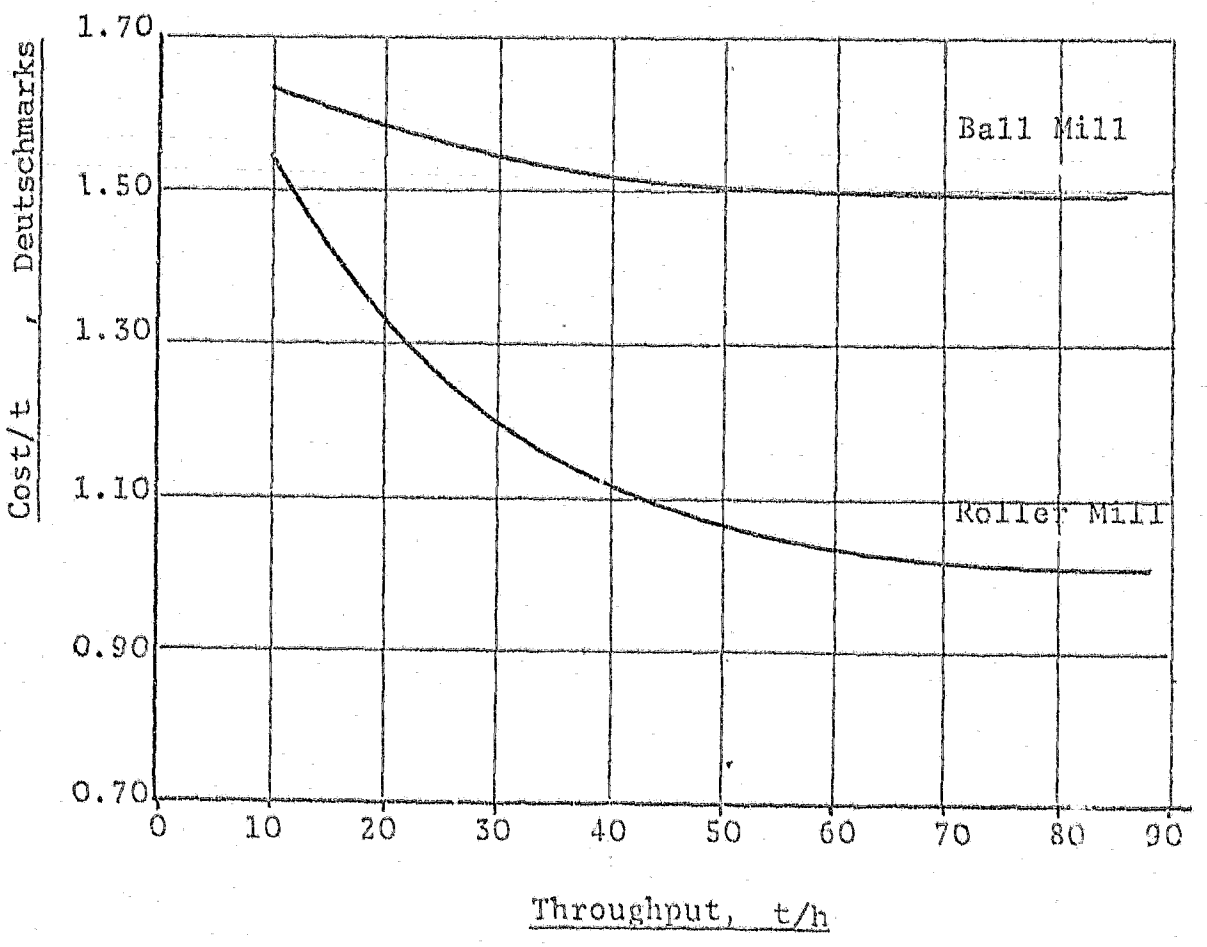

FIGURE 2,13: Throughput vs cost/tonne (from M35)

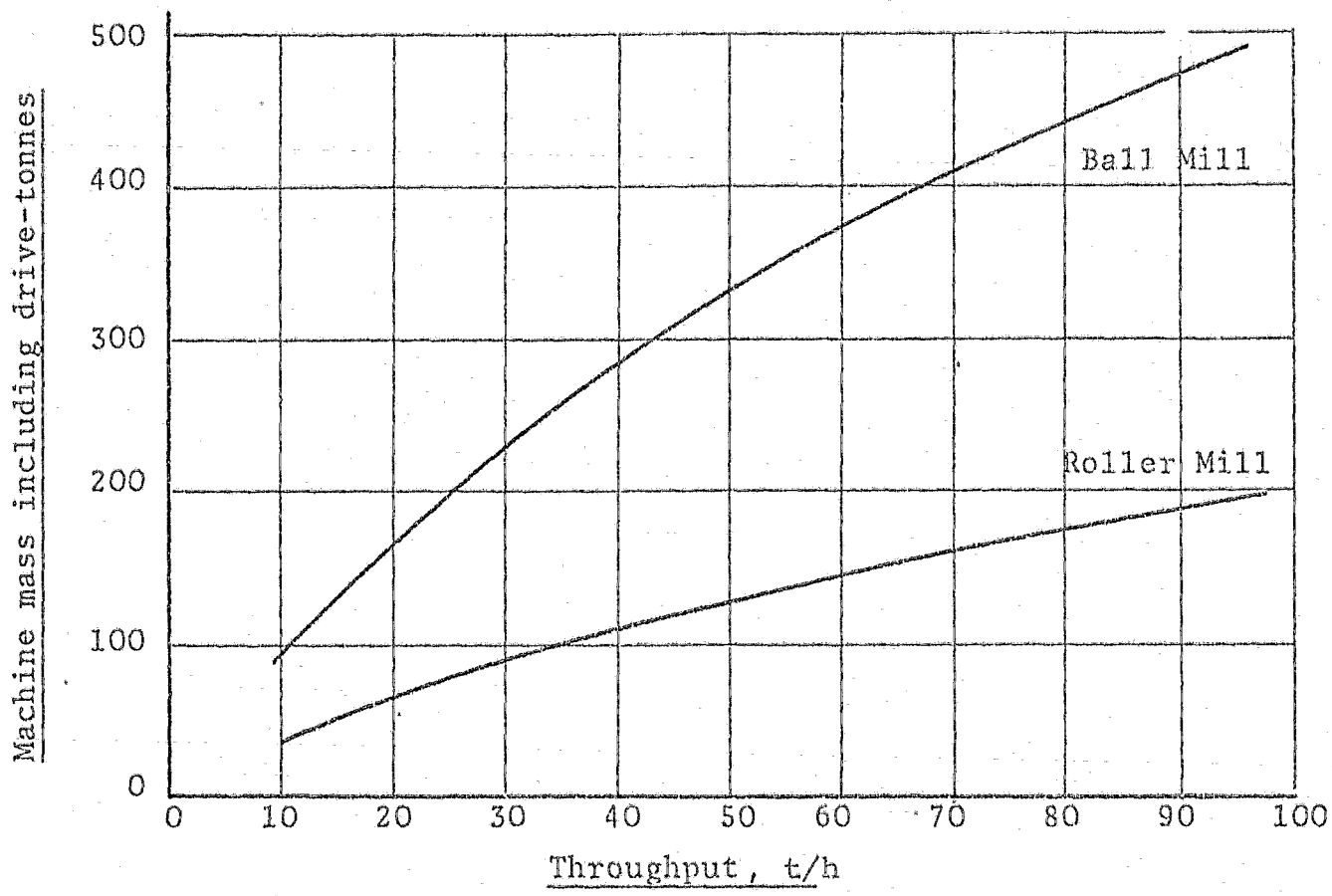

FIGURE 2.14: Throughput vs machine mass (from M35)

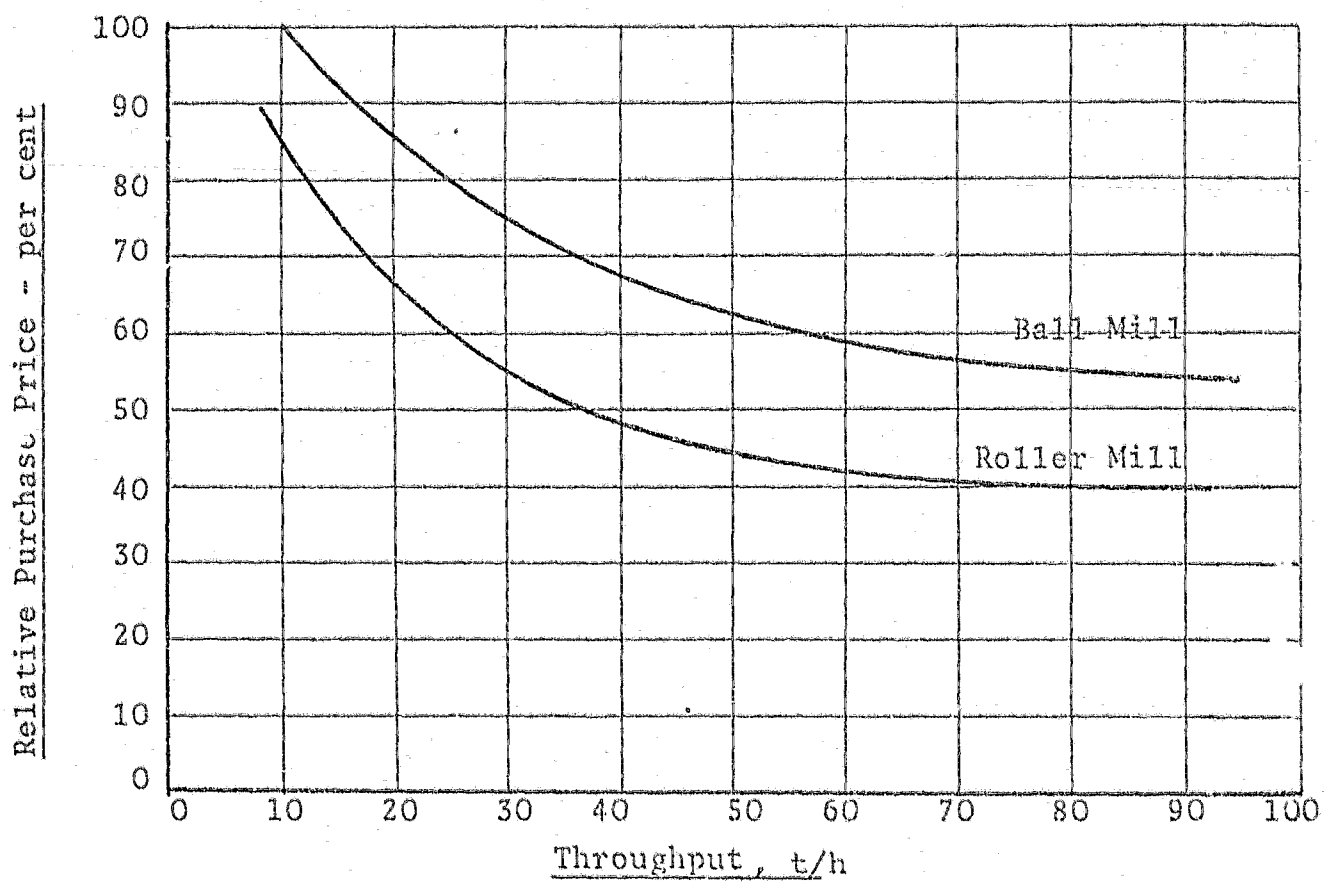

FIGURE 2.15: Throughput vs relative purchase price (from M35)

2.5.1 Open Circuit Pressure System (Figure 2.16)

Pressure type mills are used on most large modern boilers. Nearly all use the open circuit layout. A typical layout is shown in Figure 2.16. Heated air from the air heater is blown into the mill via a primary air (P.A.) fan designed for the high temperature applicaction. A seal air fan supplies clean air to all bearings and seals within the mill pressurized area.

Advantages

- The P.A. fan does not handle dust, so maintenance is low.
- The system can therefore be used where coal is abrasive, since there is no wear due to coal passing through the fan.

Disadvantages

- Special seals are required on the mill moving parts, i.e. gearbox, rolls, separator.
- A seal air fan is required.
- There is a dust nuisance if leaks occur.
- The reject boxes have to have special sealing arrangements, i.e. an inner door must be closed before removing the rejects from the box.

2.5.2 Open Circuit Suction System (Figure 2.17)

For small units handling soft coals, this system is preferred from a cost point of view.

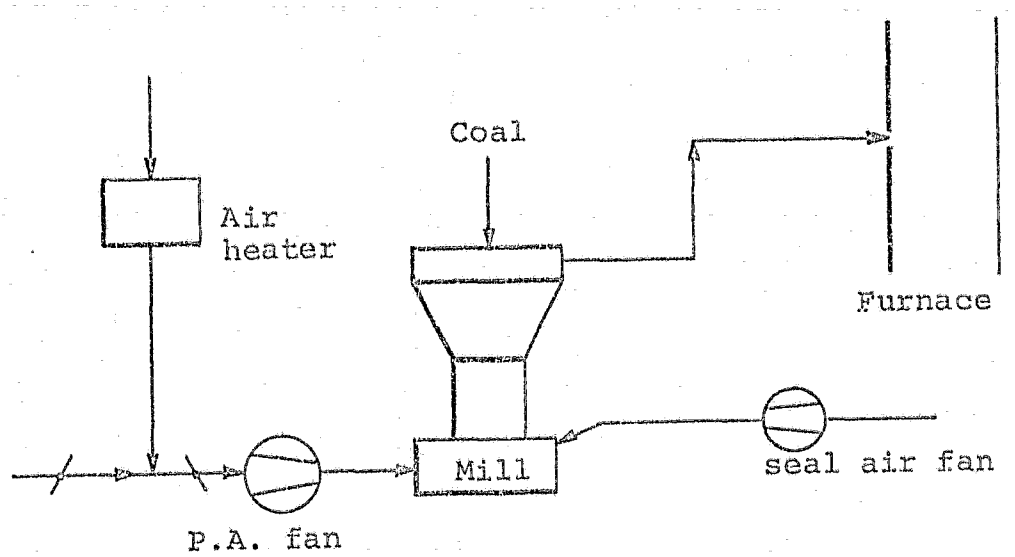

FIGURE 2.16 Open circuit pressure system

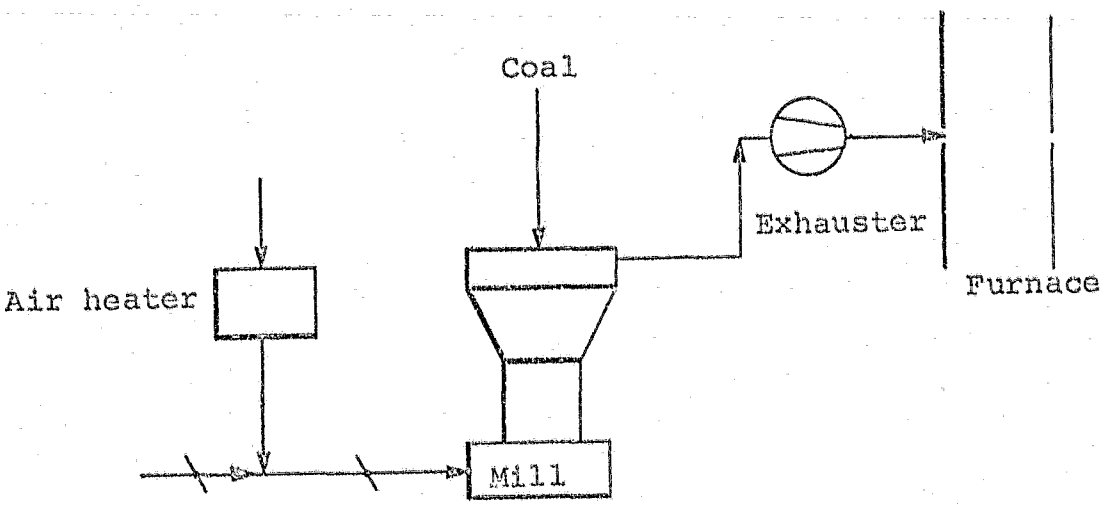

FIGURE 2.17 Open circuit suction system

Advantages

- No special seals required.
- No seal air fan required.
- Flap type reject doors are adequate.
- There is no dust when leaks occur.

Disadvantages

- The exhauster fan is prone to wear, especially with South African bituminous coals. This causes inefficiency and an imbalance of the impeller, with subsequent vibration.

2.5.3. Closed Circuit Milling (Figure 2.18)

This system is used mainly for firing kilns and installations where the mill cannot be shut down for operational reasons. A bin system is therefore used, with a 6 to 8 h storage capacity to enable maintenance to be carried out on the mill. The system utitilises the P.A. fan as a dust collector or dust draw-off point, since the cyclone is not usually more than 90% efficient in the normal type of installation. The circuit is arranged so that a slight suction exists at the mill inlet, so making a seal air fan unnecessary.

When a ball mill circuit is used, the size classification is made external to the mill, as shown in Figure 2.19. An adjustable vane separator returns oversize to the mill inlet for further grinding. The fines taken from the cyclone are drawn off to a dust collector via a fan exhausting to atmosphere. The coal collected from the cyclone and dust collector then has to be blown into the kiln by a third fan with feeder. Here

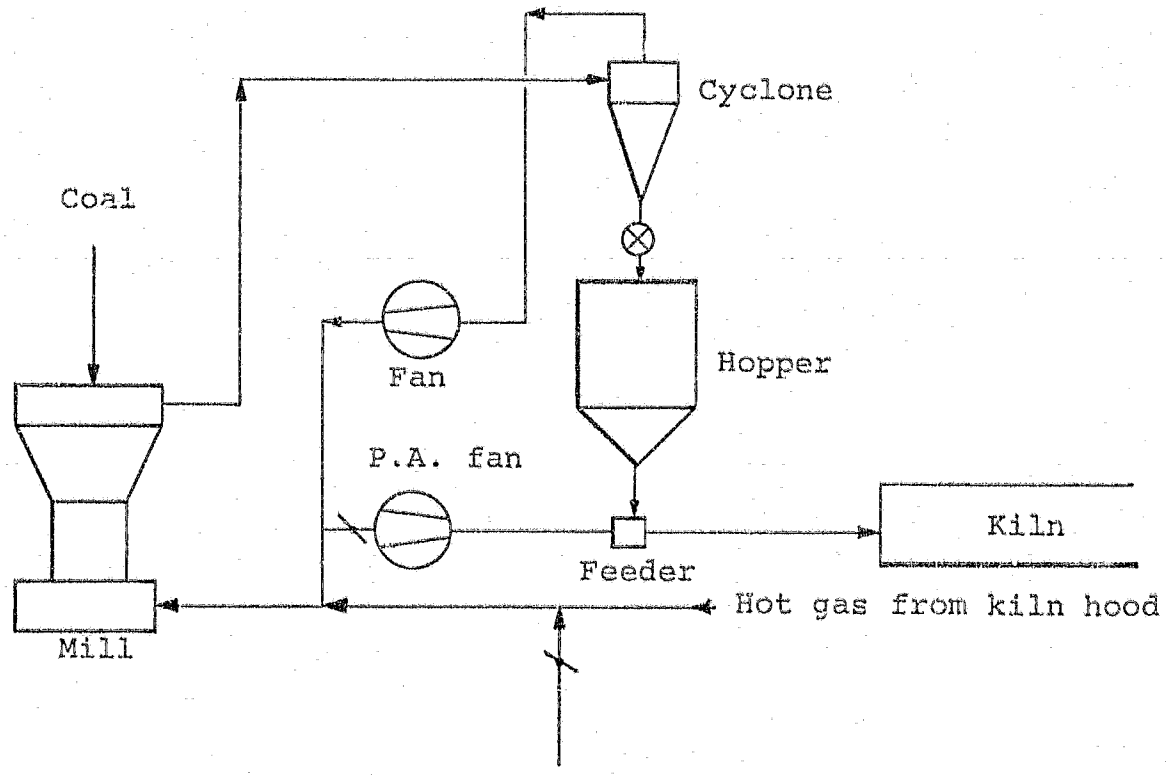

FIGURE 2.18: Closed circuit system with vertical spindle mill

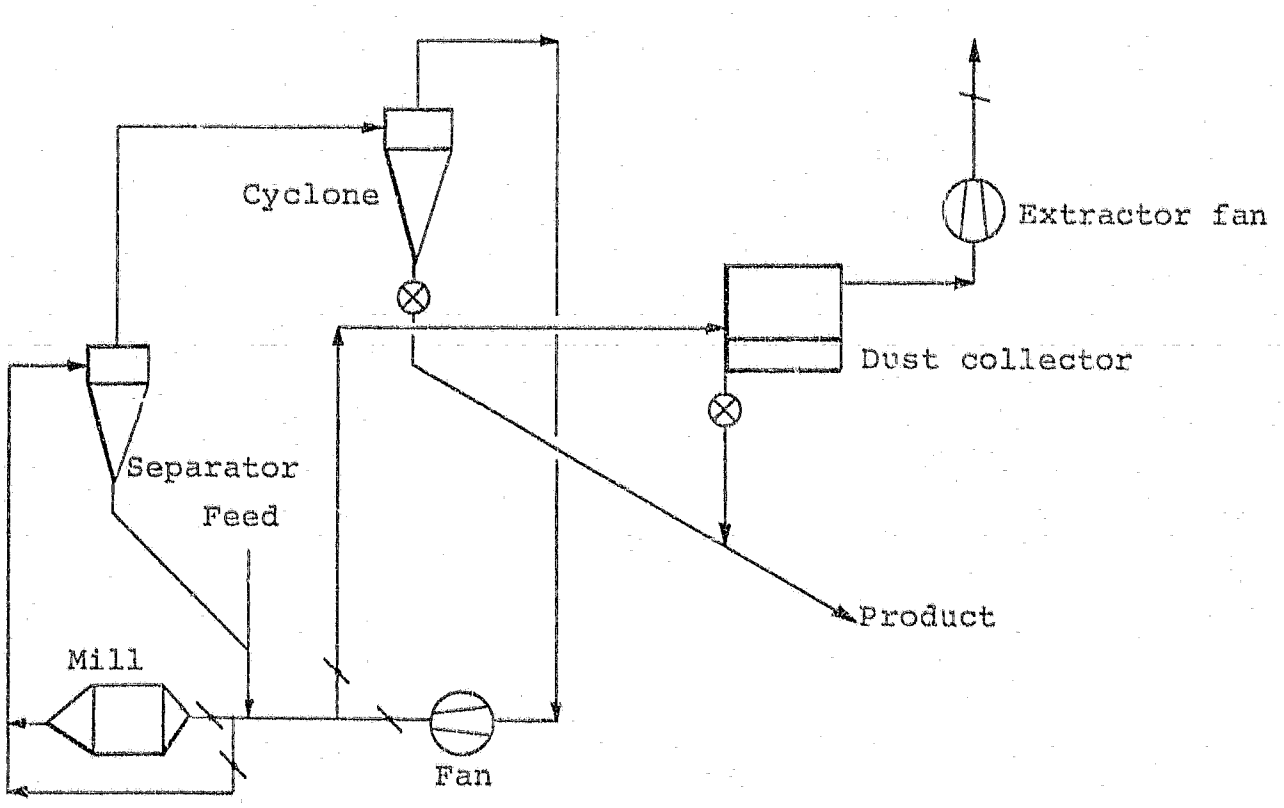

FIGURE 2.19: Closed circuit system with ball mill

again the system pressure is designed so that a slight suction exists at the mill inlet.

For drying wet feed material in a closed circuit, an air heater, either oil or gas-fired, can be located at the mill inlet where a slight negative pressure exists (Figure 2.20). The dust take-off to the dust collector must be sized to keep the relative humidity of the circulating air well below dew point.

Normally, if no heat is added external to the mill, the closed circuit temperatures reach an equilibrium value, depending on the moisture, of about 60°C due to the energy expended in the grinding action and to air friction in the system.

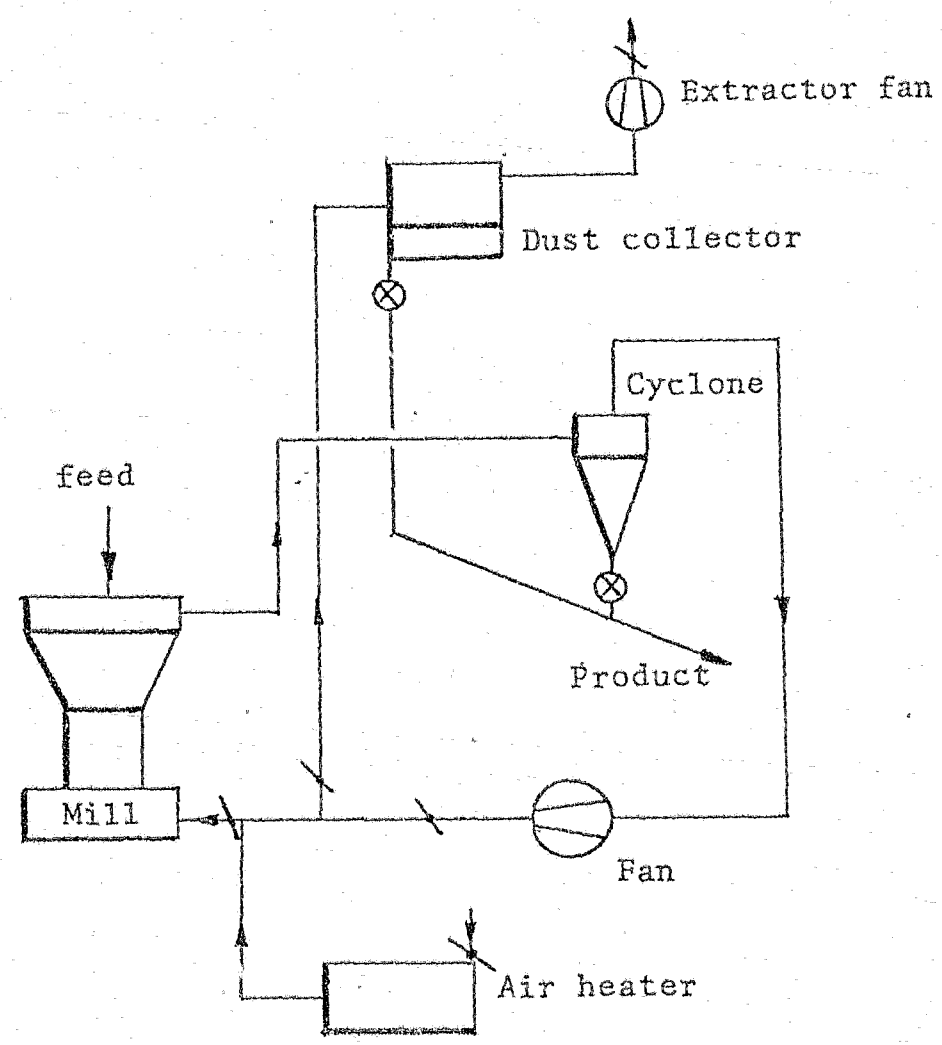

FIGURE 2.20: Closed circuit system with air heater

CHAPTER 3

SURVEY ON MILL RESEARCH FINDINGS AND ASSOCIATED PARAMETERS

3.0 INTRODUCTION

The field of investigation into milling has expanded tremendously during the last decade due to the increased use of larger and more efficient mills for a wide range of applications. As part of the investigation conducted, the author visited overseas institutions where research of this kind was being carried out in order to gain first hand information about various aspects of milling, with particular reference to coal milling. This survey outlines briefly some of the more important investigatory aspects which will be discussed in the light of actual data obtained in subsequent Chapters.

3.1 MILLING AND MILLING TESTS

In 1954 the British Coal Utilisation Research Association (B.C.U.R.A.) conducted extensive tests (M16, M17) on a ring ball mill to establish parameters and equations for plant performance. Some of the pertinent conclusions were:

- Maximum fines output increased with ball track pressure.
- The maximum recirculating load was estimated to be up to ten times the output.
- The major portion of the mill pressure drop occurred in the throat area whilst the separator pressure drop was negligible.

- The hot air leaving the throat gave up its heat in drying coal while travelling only 25 mm after mixing, and temperatures throughout the rest of the mill were substantially uniform.

- The Hardgrove Index may be taken as a guide to performance for this type of mill.

- For a given output of fines, the power required was dependent to some extent on the method of operation of the mill. Hence only broad relationships could be defined between mill power, output and fineness.

Since the Hardgrove Index has been taken as a standard for assessing coal hardness, it is useful to outline here some of the findings on investigations carried out by B.C.U.R.A. and the Fuel Research Station on the Hardgrove machine which is similar in principle to the ring roll mill used by B.C.U.R.A. in the tests referred to above:

- B.C.U.R.A. managed to reach an index standard error of 0.2 by rigidly adhering to the correct laboratory procedures. A laboratory at a relatively steady temperature was essential for precise work.

- A relationship between percentage undersize D(x) and particle size x from the Hardgrove machine was found to be of the form

$$D(x) = K_1 x^{\gamma}$$

where K_1 and γ depended on the type of coal. It was concluded that the size distribution of the product from Hardgrove tests should conform to a consistent pattern.

- Different methods of sample preparation could affect the Index.

Fitton and Hughes (M7) compared the Hardgrove test with the ASTM ball mill test. Figure 3.1 shows the correlation obtained.

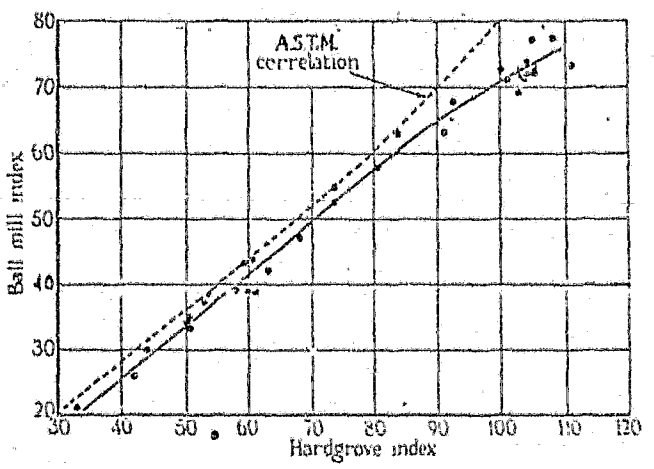

FIGURE 3.1: Correlation of Grindability Indices (from M7)

Some of the more interesting findings were:

- Different types of sieving machines could give different sieving characteristics.
- On the British coals studied the grindability measured an inherent property of the coal related to (a) the nature of the coal substance and (b) its physico-chemical properties.

- The Hardgrove Index remained constant for a sample having a moisture content of 0 to 11%. Drying the coal below its normal air dried moisture content increased the grindability of a low and high volatile non-caking coal, but did not alter that of caking coal.

- The Index was a reliable guide to the rate at which fines could be produced.

- There was a fairly close correlation between Hardgrove Index and ball mill Grindability Index over a wide range of British coals.

Mill tests by McKenzie et al (M22), also on a ring roll mill, were conducted to determine the air/coal flow pattern around the grinding ring by using a mock-up slice model and by visually observing flows. By varying the throat geometry it was found possible to bring about a 20% increase in mill capacity and a lower pressure loss. During this investigation, mill voidages were measured using a pitotstatic probe and a radioactive probe in the dense air/coal mixture at the throat. The gamma ray absorption was found to correlate with the density of the fuel bed between the source and the counter of the probe, and some results are shown in Figure 3.2.

As the correlation between the two types of probe was so good, the pitot-static pressure probe was used for further tests as a result of its simplicity. The voidages were calculated from the formula for pressure drop across a fluidized bed:

$$\Delta P = L \rho_s (1 - \varepsilon) g$$

The low voidages measured are indicative of a settled bed and some doubt must exist as to their accuracy.

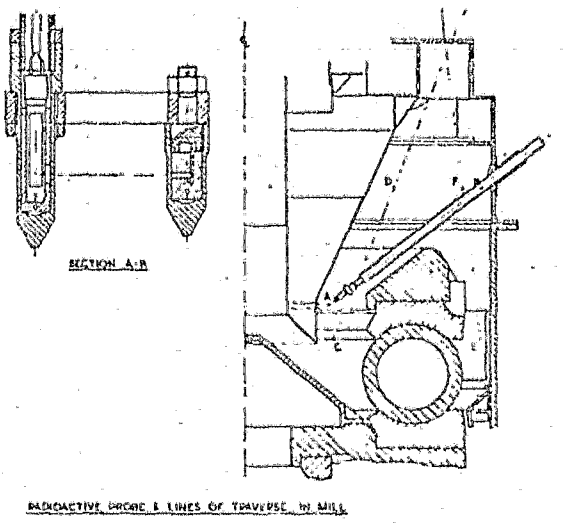

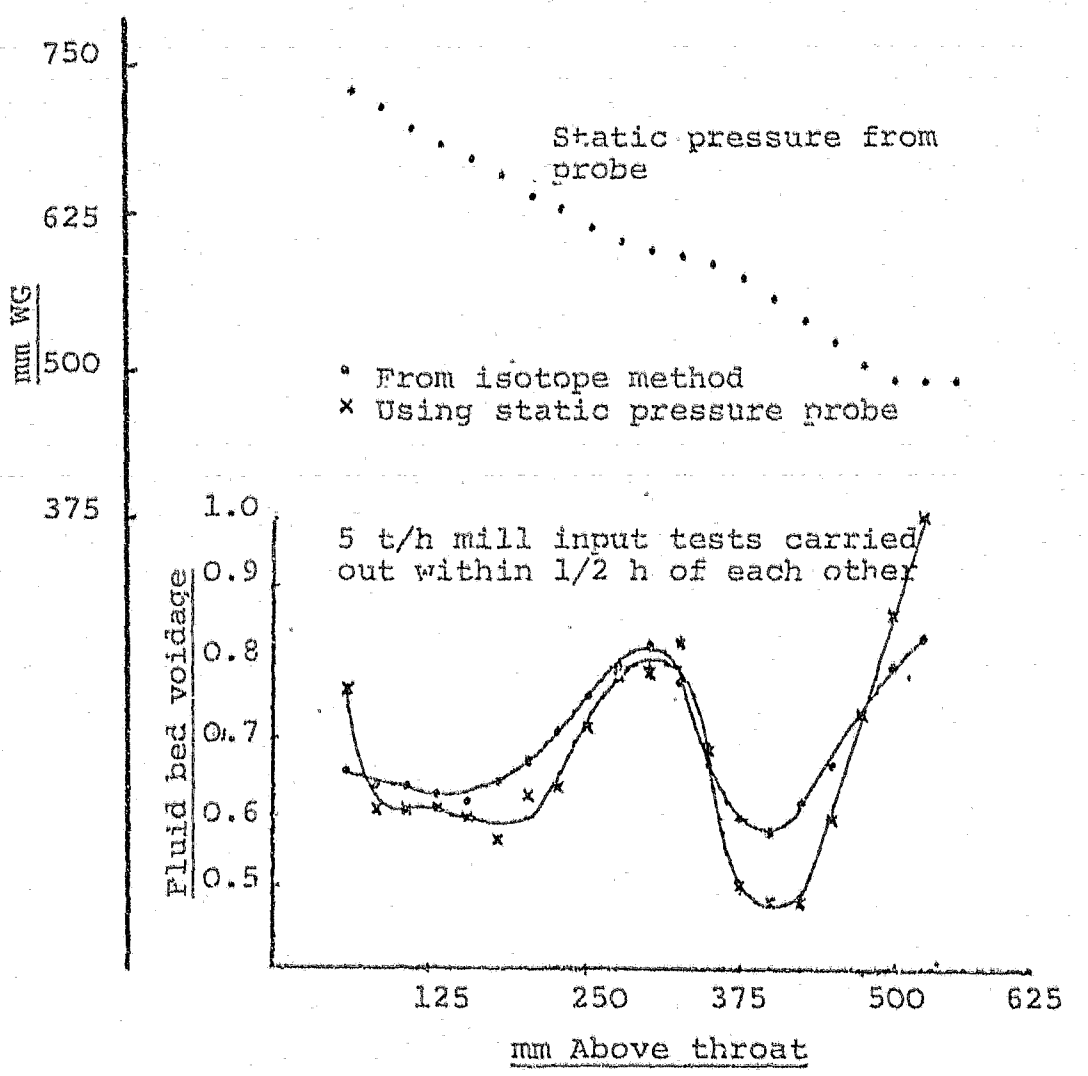

FIGURE 3.2: Voidage measurements on a ring roll mill (from M22)

Concurrent with the mill investigation, a testing programme of static separators gave the correlations shown in Figure 3.3.

Kiselev and Kondrat'eva (M20) tested roller mills in various Soviet power stations to determine the dependence of table coal layer thickness, number of roll passes, roll speed, and feed to the roll on mill performance. An interesting observation was the reduced specific power consumption when the rolls were driven with separate electric motors, as compared to the customary method of driving the table.

Various roll geometrics have been tested by the Central Electricity Generating Board (C.E.G.B.) but no published data is available. The roll cone angles tested were 45°, 25° and 15°, and it appeared that the 45° and 25° angles gave a more efficient grinding action on a once-through basis. This institution has also conducted work on classifier efficiencies using irradiated coal, and measuring the Na gamma radiation, thereby determining the cut size (Figure 3.4).

The application of ball mills for coal grinding is not as popular now as formerly, due to higher running costs, slow control response and the amount of floor space required. However, the fundamental laws governing the operating parameters have been studied extensively.

Rose et al (M28) used dimensional analysis to derive working equations for a ball mill and the work of Bond (G4) is also well known.

INDEPENDENT VARIABLE / DEPENDENT VARIABLE	INLET VELOCITY Vi	PRODUCT QUANTITY TP	PRODUCT GRADING G	BLADE ANGLE Θ
PRESSURE LOSS ΔP	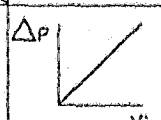			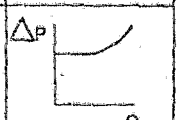
CLASSIFICATION EFFICIENCY η	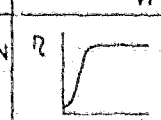	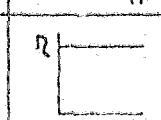	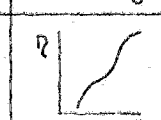	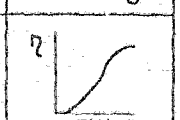
INDEPENDENT VARIABLE / DEPENDENT VARIABLE	OUTLET SKIRT DEPTH S	AIR TEMPERATURE T° ABS.	CLASSIFIER SIZE Di	
PRESSURE LOSS ΔP	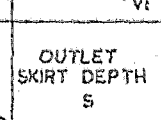	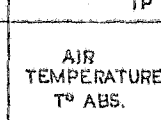	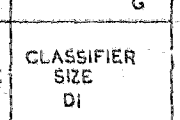	
CLASSIFICATION EFFICIENCY η	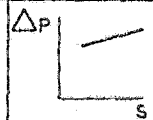	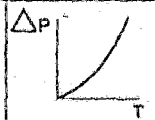	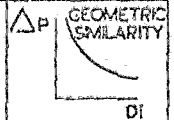	
EACH CHARACTERISTIC REPRESENTS THE EFFECT OF THE STATED VARIABLE ONLY, WITH ALL OTHERS HELD CONSTANT.				

FIGURE 3.3: Separator characteristics (from M22)

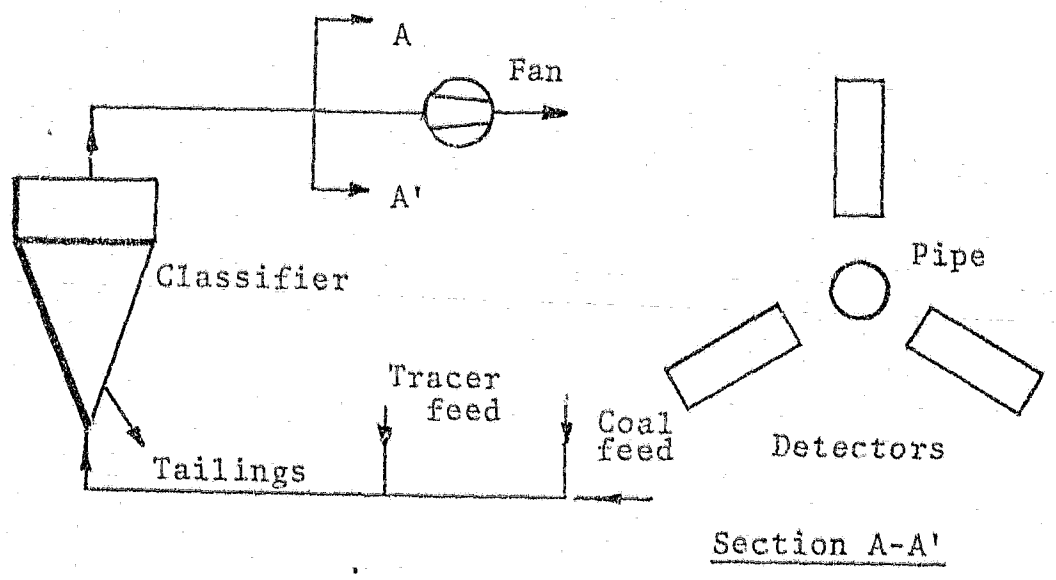

FIGURE 3.4: Typical classifier test layout

Results from Komati Power Station on ball mill tests by Messerschmidt (M23) showed the effects of ball charge, volume filling and operating parameters on fineness and power. The 52 mesh coal residue and 52 mesh grits residue were almost directly related, indicating the importance of minimising this size fraction in pulverised fuel if high efficiencies are to be maintained.

Messerschmidt's (M24) theoretical paper on the air/coal flow dynamics within a vertical spindle mill brought out the following points:

- The static pressure drop across the mill due to coal burden was a direct indication of the volumetric concentration within the mill.

- The maximum volumetric concentration that could be kept in suspension in any part of the mill increased as the vertical air velocity in the bed increased or particle size decreased.

- For optimum reject behaviour the maximum volumetric concentration must be approached, with the resultant high air velocity in the bed.

Generally, the information available on mills is confined to a particular type for which parameters are worked out, and a general trend is often the only means of correlating otherwise complicated parameters. For this purpose, model milling circuits have proved valuable in establishing scale factors for new development both in size and performance. In this regard, International Combustion tested mill models to assess the pressure drop through lourvres, and the effect of table speed and table ploughs on coal flow across the table. Classifiers were also tested using wood chips as a tracer (M12, M13, M14).

3.2 WEAR IN MILLS

Due to the nature of the grinding process, it is to be expected that large wear rates will be found under certain conditions of service. Mills are therefore designed to cope with the problem, and use is made of easily replaceable parts to minimise breakdown maintenance and to extend the life of the mill. Examples of these are roller tyres, table segments and body protection plates and liners, the former two being made of a Nihard or similar metal with high surface hardness, the liners being of mild steel.

As explained in subsequent Chapters, the mill rejects some debris, but it is the remaining fraction that causes the damage when it is swept up into the mill by the high velocity air at the table throat. Gibbings (W5) performed dimensional analysis on the wear by particle impact of fluid flows, and arrived at the following relationship:

$$\frac{\dot{m}s}{\rho^2 d^3 v^3 L^2 C} = F(\rho_s/\rho_f)$$

The interpretation of this relationship is as follows:-

- Wear rate is proportional to the cube of velocity.
- Wear rate is proportional to particle volume (or length cubed).
- Wear rate is proportional to concentration (for low concentrations).
- Wear rate is proportional to the square of the size of the flow system.

Considerable work on the wear by coal and its associated constituents has been undertaken by the B.C.U.R.A. Parish and Beaman (W10) compared wear rates against Abrasive Index (using the Yancey,Geer and Price method as described in the appendix) by passing the coal between two spring loaded rollers, one of which had an activated ring in its grinding surface. The radioactive debris in the crushed coal was measured, and a direct relationship obtained between wear and coal properties. Similar tests on shale indicated that the wear was caused by its quartz content. The particle size of the quartz particles also proved to be an important feature; wear increased with particle size up to at least 250 μm.

It is obvious that economics dictates to a large extent whether it is more profitable to remove as much reject material as possible, or to refurbish mills more often. A point often overlooked in this respect is the not so obvious extra cost of inefficient operation when rolls and table segments are worn, resulting in poor fineness, higher power consumption and lower boiler efficiency. Tests conducted by Messerschmidt at Camden Power Station revealed very slight wear reduction with reject increase (Figure 3.5). In any event, the amount of rejects was only a fractional percentag of the tonnage going through the mill.

To illustrate how wear affects mill performance, Figure 3.6 has been derived. This is based on experimental work, hence it is most important when sizing a mill to allow for wear, especially when guarantees have to be met.

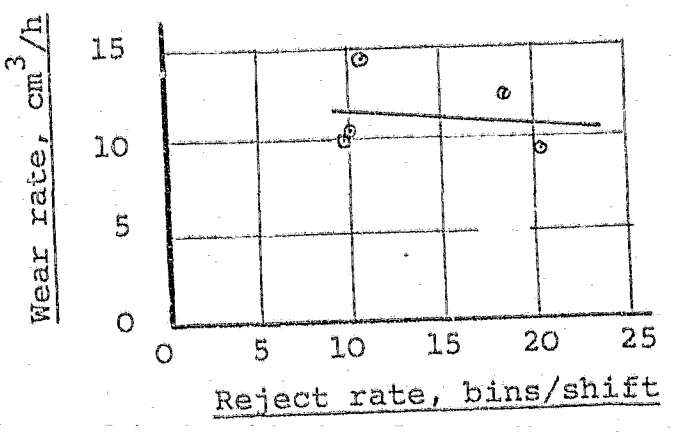

FIGURE 3.5: Wear rate tests (from W11)

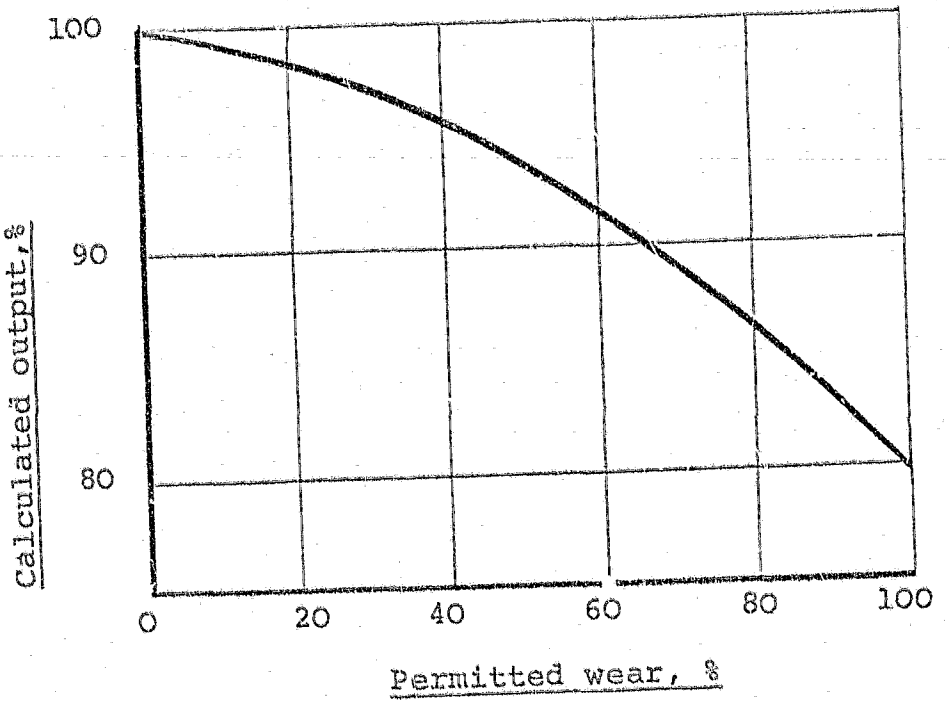

FIGURE 3.6: Mill output vs roller and table wear (from M35)

Tests conducted by I.C.L. at Blyth Power Station (W8) were aimed at establishing wear comparisons between a laboratory sized LM 1.6 mill and an LM 16/3 mill operating on the same coal under controlled conditions. The wear was measured on the table and the rollers. The wear rates in a Raymond laboratory mill and on a Yancey, Geer and Price (Y.G.P.) machine were also measured using coal samples selected from the mills, and a comparison of all four wear rates was drawn up. It was concluded that the Raymond and Y.G.P. methods were not reliable enough to predict the life of the wearing parts of a commercial mill, and even the comparison between the two mills, i.e. LM 1.6 and LM 16/3, only showed a trend, and could not be used to accurately predict commercial mill wear rates.

Of special note is the graph of Figure 3.7, showing the close relationship between percentage alpha quartz and wear. This method could offer a fairly accurate means of determining alpha quartz content once a basic curve has been experimentally established.

Figure 3.8 indicates the amount of scatter to be expected from the laboratory wear tests as compared to the commercial mill wear rate tests. The Y.G.P. method has been the standard procedure adopted by South African power station personnel in assessing the relative wear likely to take place in a mill, and although a trend is here evident, there is apparently a large inconsistency present. This method is not recommended as a direct comparison for roll or table wear, but rather as an overall maintenance-cost comparison.

Figure 3.9 shows the high quartz content remaining on the mill table after a mill shutdown - apparently remaining there due to its higher density and resistance to grinding.

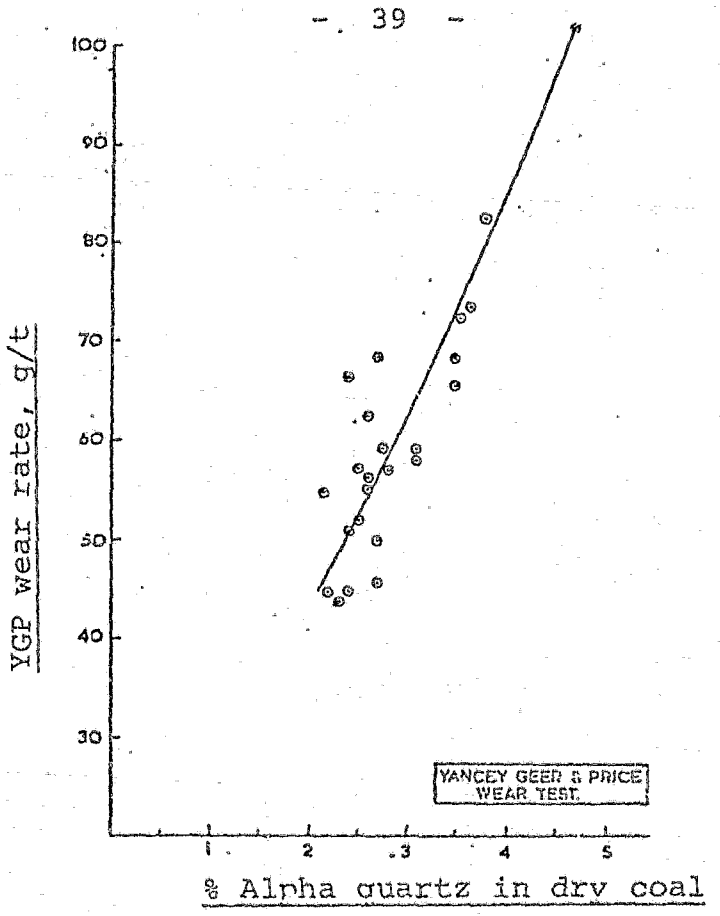

FIGURE 3.7: Wear rate in Yancey Geer and Price test

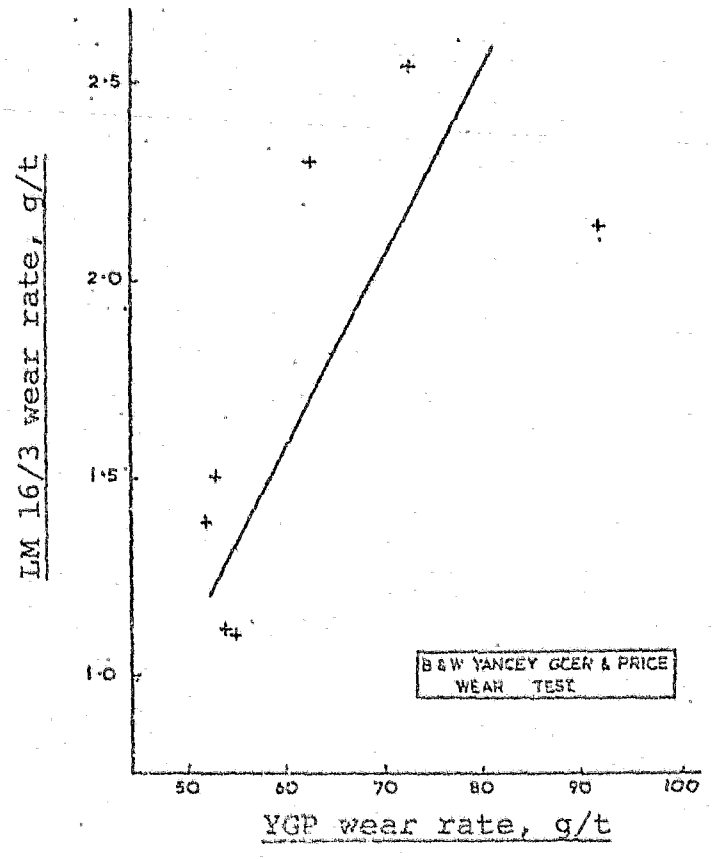

FIGURE 3.8: Mill and labora wear rates

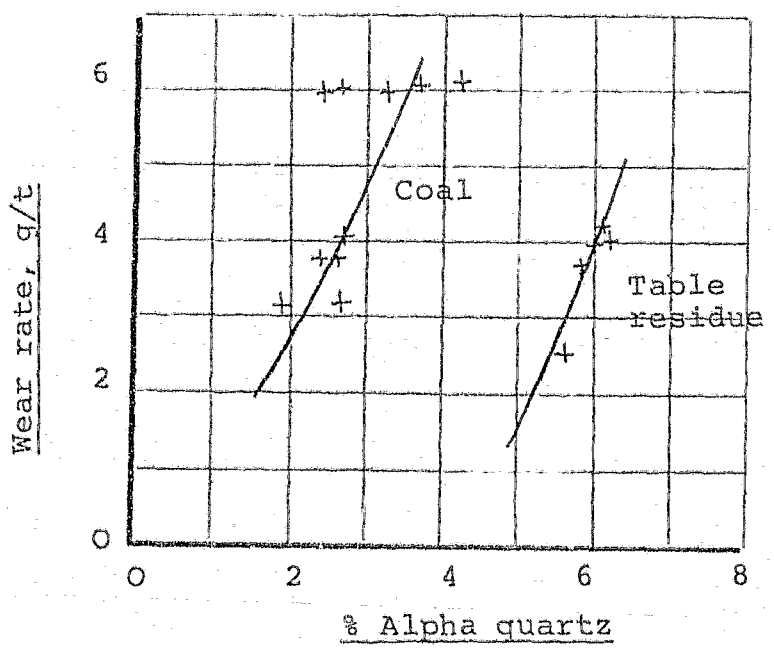

FIGURE 3.9: Alpha quartz in coal vs wear rate for LM 1.6 mill (from W8)

The table residue is responsible for increased roll and table wear and methods should be adopted to clear as much of it away as possible during mill operation.

3.3 COMBUSTION

The performance of the pulverizing plant in grinding the coal to the correct size range is important with regard to the combustion and efficiency of the overall boiler plant. Factors such as burn-out time, residual carbon-in-ash, and the deposition of slag on various parts of the combustion chamber all affect the unit performance and are directly caused by the method (velocity range, burner tilt) and quality (pulverised fuel temperature, sieve size range) of pulverised coal introduction into the furnace.

Burn-out phenomena have been studied by numerous researchers for both single particles and dust clouds. The general relation for single particle burn-out time was found to be:

$$t = r_s^2$$

It was found by Katsnel'son and Marone (C2) that the ignition time of a dust cloud decreased with increasing volatile content, but that the magnitude of this effect was governed by particle size, i.e. for very small particles an increase in volatile matter had very little effect.

Shagalova *et al* (C2) used solid sampling techniques on a steam boiler to investigate the burn-out of anthracite dusts. They found that the smallest particles of the cloud burnt away first and that the time required for

combustion of 90% of the anthracite was 20 to 25% of the time for burn-out of 98% of the anthracite. The compiled data on the burn-out of various types of coal all show particle size as a prime parameter, and therefore this has been the main controlling function when firing a boiler at the highest efficiency.

3.4 PARTICLE SIZE DISTRIBUTION REPRESENTATION

The comminution process as used industrially is largely uncontrolled as to the selection of particles for grinding or breakage. A mill is fed with a material of size distribution determined by previous reduction, scalping or classification, and this is based on a statistical distribution or frequency curve peculiar to that particular process. Similarly, the particles ground in the mill are not presented in any set order to the rolls, so that one would expect a random distribution of material for size reduction under the rolls. This ground product is then classified, the oversize returned for further grinding, and the undersize discharged from the mill. It will be seen that throughout the process the controlling feature is the classification action which can be predicted.

Related to the representation of a mass size distribution is the actual problem of defining particle size. Obviously it would be impractical to measure individual particles for surface or volume and to calculate an average spherical particle therefrom. The standard approach is to use screens with square openings (meshes) and by so doing to separate the sample into various size ranges. If the particle mass falling within the sieve ranges is plotted against the sieve size x, a histogram will result, the curve tending to a continuous line for small and

constant intervals of x (Figure 3.10). If the masses of the individual sieve residues (as a percentage of total sample mass) are plotted as a cumulative curve, this will indicate either the retained mass or the passing mass, i.e. R(x) or D(x) (Figure 3.11). Clearly

$$R(x) + D(x) = 1.$$

The laws governing the size distribution of a ground or crushed media were expounded in empirical terms by Rosin and Rammler (P14) in 1931, and related to experiments carried out by those authors on a large selection of materials. Considering screen residues $R(x)_A$ and $R(x)_B$ for sieve sizes x_A and x_B, they found that

$$R(x)_A = 100\ (R(x)_B/100)^{(x_A/x_B)^n}$$

from which

$$R(x) = 100\, e^{-bx^n} \qquad \ldots\ldots\ldots\ldots\ldots\ldots\ldots\ldots (3.1)$$

This can be rearranged to give:

$$\log \log (100/R(x)) = n \log x + \log b + \log \log e$$

This of the form y = mx + c, i.e. a straight line. Clearly, if log log 100/R(x) vs log x is then plotted, n is the slope of the resulting line, and log b + log log e the intercept on the ordinate. Tests have confirmed that this law is valid irrespective of type of coal, type of mill, or method of classifying, while in the case of a ring roll mill, the exponent n increased with increased fineness. Since this law follows that of probability, greater discrepancies

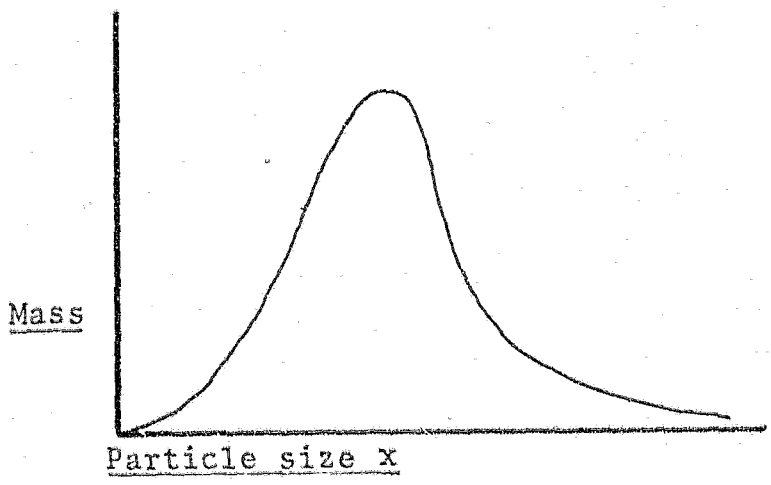

FIGURE 3.10: Particle mass histogram

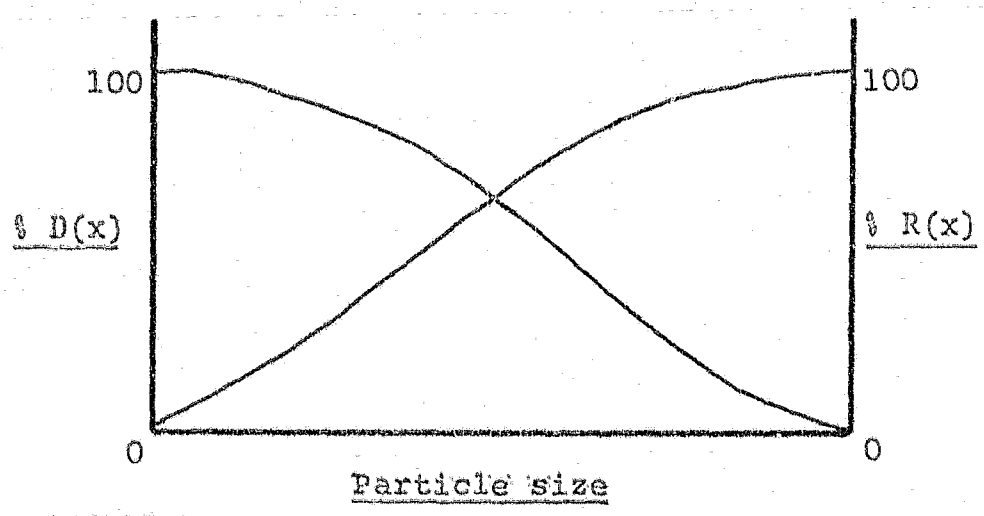

FIGURE 3.11: Particle mass cumulative curve

can be expected with the coarser sieves than with the smaller particles, and for this reason the 100 mesh and 200 mesh will be more reliable than, say, the 44 or 52 mesh when dealing with typical pulverised fuel powder.

The Rosin-Rammler (R-R) plot - representing equation (3.1) above - has been used extensively by researchers in the milling field and all size relationships presented here will be based on these curves, since their suitability has yet to be disproved for coal milling applications.

Equation (3.1) was subsequently modified by Bennett (G3) by substituting $(1/x_o)^{n}$ for b, giving

$$R(x) = 100e^{-(x/x_o)^{n}} \quad \ldots\ldots\ldots\ldots\ldots\ldots\ldots\ldots\ldots\ldots (3.2)$$

This modified approach gives $R(x) = 36.8\%$ when $n = 1$ and $x = x_o$.

Beke (M2) termed n the uniformity coefficient and x_o the absolute size constant or characteristic particle size. Lower values of n are associated with a more scattered distribution, whilst higher n values represent a more uniform particle structure.

Figure 3.12, which represents a typical material sample size plotted on R-R graph paper, shows how sensitive the residue is to variation of slope. For a residue of a given size of, say, 70%, corresponding residues for other size ranges will vary markedly if the slope is changed. n is therefore a pointer to the type of grinding taking place, i.e. a wide or narrow size

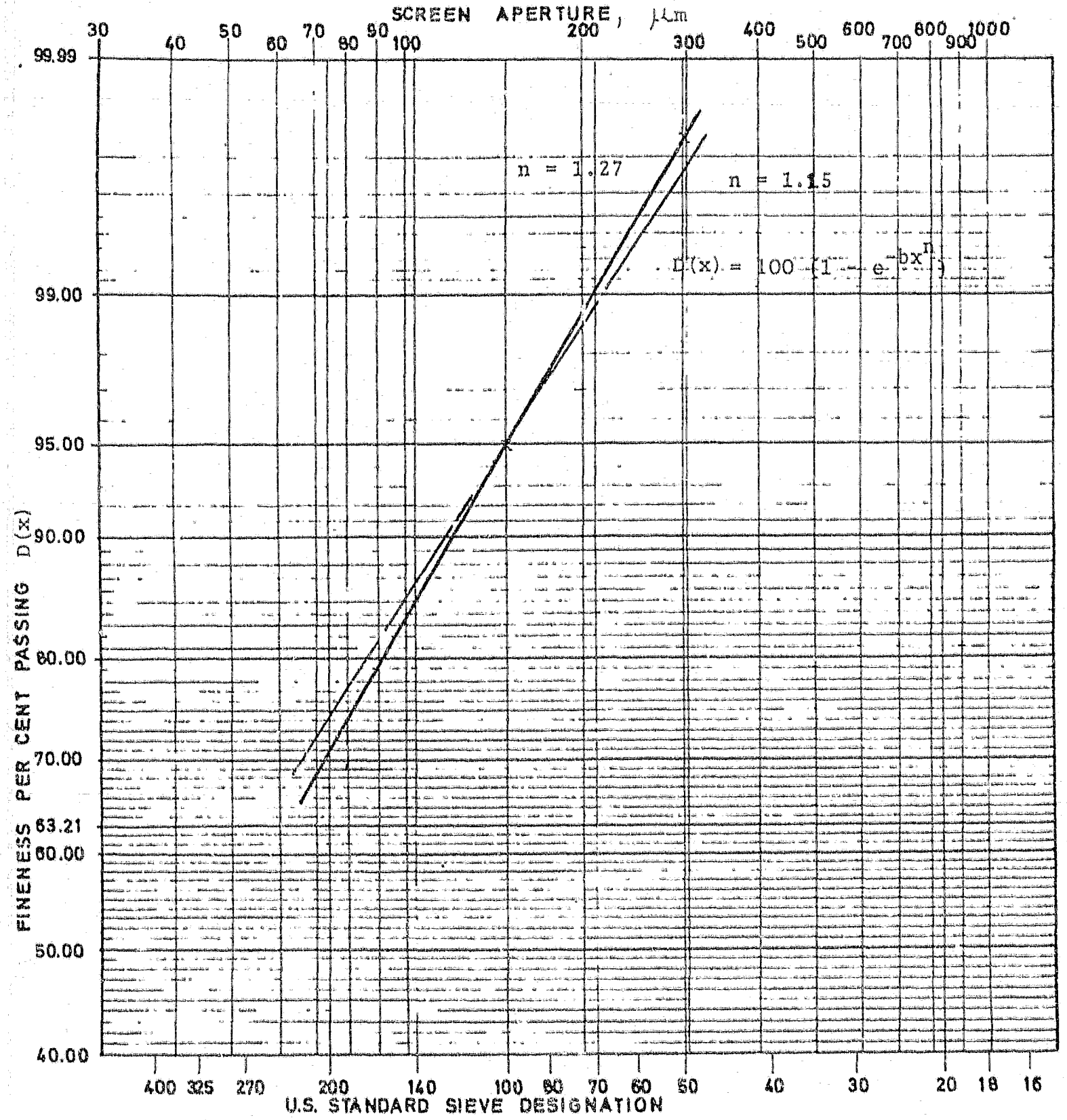

PLOT OF ROSIN AND RAMMLER EQUATION FOR USE WITH PULVERISED COAL

FIGURE 3.12: Typical p.f. sample distribution
(Arnot Power Station test data)

distribution, as well as a trend indicator for changing parameters.

The applicability of the R-R equation has been in the finer size ranges down to 1 μm. For coarser particle sizes the curve tends to bend at the coarser end. This is to be expected as larger particles, although fewer in number, make a disproportionate mass contribution to the overall sample mass and hence the cumulative distribution. It is, however, interesting to note that the equation does apply to coal obtained by blasting (M2).

A detailed analysis of the R-R equation is given by Beke (M2), wherein it is stated that the surface and number of particles cannot be accurately determined using the R-R correlation, owing largely to variations in magnitude of the uniformity coefficient n. However, the present use of this equation does not make use of Beke's additional parameters.

Besides knowing the distribution of the particles on a mass basis, it is also useful in grinding operations to be able to assess the grindability, or average particle size. This will give an indication of the efficiency of the operation, especially when considering it on a time basis (i.e. for a batch grinding process). Beke analysed the Bennett equation (equation (3.2)) to represent standard deviation and the geometric mean of the distribution by means of the following equations:

Standard deviation $\sigma = \pi / \sqrt[n]{N6}$

Geometric mean $A_g = x_o / \sqrt[n]{1.781}$

Geometric mean

Haywood (M2) used as abscissa the centre of gravity ordinate of the particle distribution curve to define the mean particle size x_m. If y is the ordinate of the particle distribution curve, this gives:

$$x_m = 1/100 \int_0^\infty xy\, dx = 1/100 \int_0^\infty 100\,\eta b x^\eta e^{-bx^\eta} dx$$

$$= \frac{\frac{1}{\eta}\sqrt{(\frac{1}{\eta})}}{\sqrt[\eta]{b}}$$

For $\eta = 1$, the mean particle size is at the point where the plotted Rosin-Rammler curve cuts the 36.8% residue line.

A further correlation, attributed to Gaudin-Schumann (M2) is worth noting here since this is used extensively in the United States. The equation is:

$$D(x) = (x/K)^M$$

Taking logarithms gives

$$\log D(x) = M (\log x - \log K)$$

which gives a straight line on a log-log plot. The value of M varies from 0.5 to 1 in practice, but variations of M $\gtrless$ 1 seriously affect distribution. The graph also has a cramped ordinate scale in the 80 to 100% passing range whereas the R-R plot is expanded in this region and hence more accurately plotted. Beke suggested that this equation's validity be restricted to the medium size ranges as the limiting curve values are contrary to experience.

3.5 PULVE'ISED FUEL MEASUREMENT

In grinding applications the final product size is usually of importance from the point of view of the following stage of utilisation. There are instances where 1% variation is all that can be tolerated, and to control to such a degree, sampling and distribution procedures must be extremely reliable. For this reason the isokinetic sampler described in the Appendix was developed for the power industry, and has been adapted for use in other fields.

3.5.1 Sampling Procedures and Flow Measurement

Apart from the isokinetic and I.C.L. probe samplers (see Appendix), various other methods intended for quick and reliable sampling have been tried out.

Snowsill (P19) developed an experimental rotating probe provided with nozzles, which sampled at the centres of equal concentric areas within a pulverised fuel pipe whilst being rotated through 360°. Whilst it sampled the whole pipe area, problems were encountered in operating it in pressurized lines.

Hemeon and Haynes (P19) showed that when sampling at velocities greater than the gas velocity, the errors in respect of size analysis were small, so this principle was used with the rotating sampler. In this regard, the influence of the dust loading on the pitot-static reading was investigated, but no appreciable error was found by using the dust/air density for estimating velocity up to 40 m/s (75% minus 200 mesh dust). (Figure 3.13).

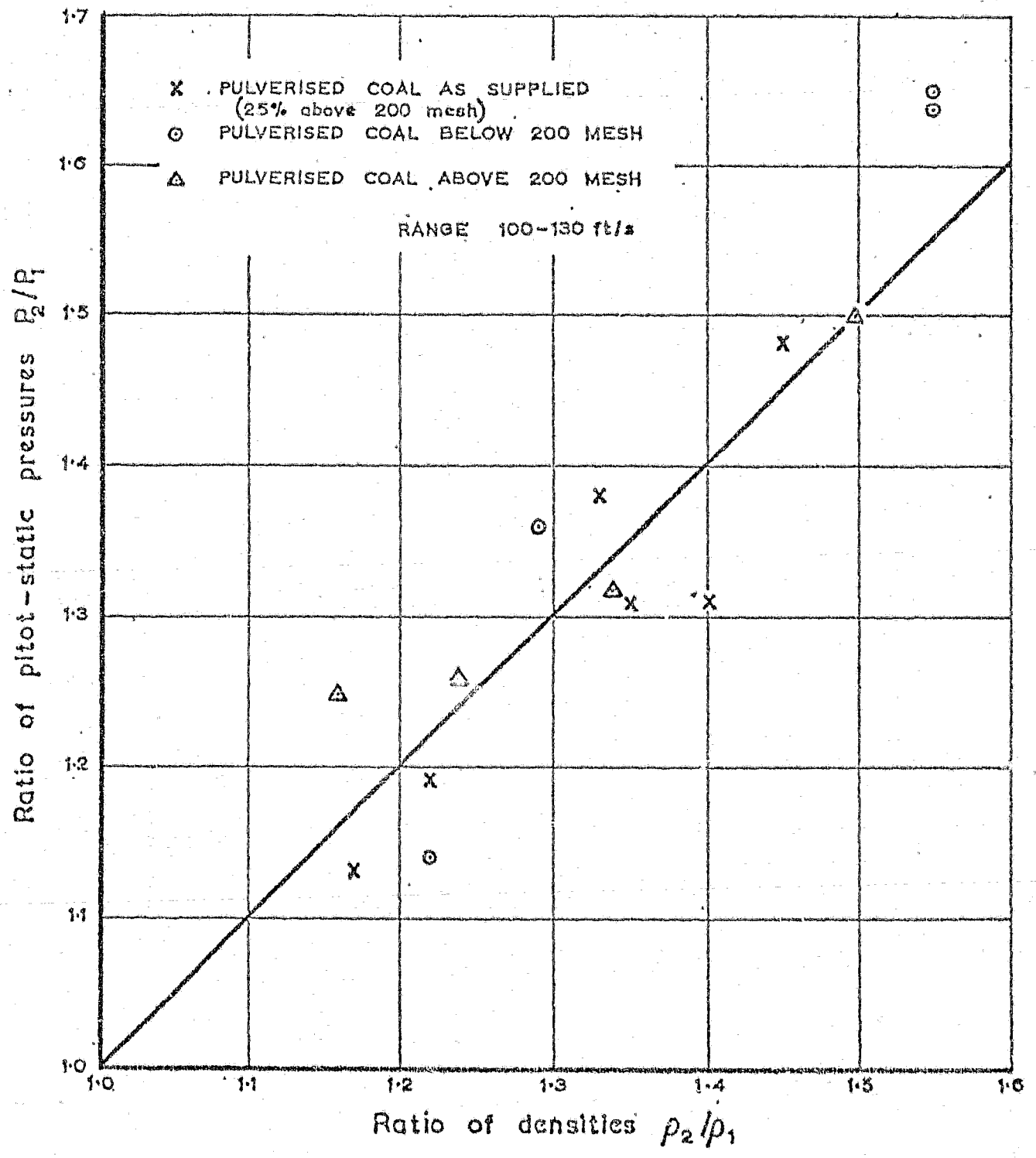

FIGURE 3.13: Relationship between pitot-static differential pressure and density of dust-air mixture (from P2)

Boals (P1) conducted sampling tests over an extended period to determine repeatability and fineness limits: the -200 mesh repeatability variation was 0.25% compared with the +50 mesh repeatability variation of 6.7%. Considering fineness, grinding consistency and repeatability, the overall variation was: + 50 mesh $\pm$ 40%; + 200 mesh, $\pm$ 16%; - 200 mesh, $\pm$ 4.9%. This is in line with the Rosin-Rammler probability curve discrepancies noted above.

The measurement of the flow rates of dust/air mixtures has not met with much success. The pitot traverse is only suitable for air quantities and the probe is often blocked by dust. By withdrawing a sample isokinetically, the flow rate can be determined, but this technique is open to the same errors as the use of static sampling points, especially when the flow pattern is constantly moving within the pipe. The pulverised fuel measurement references describe various conventional measuring techniques.

Figure 3.14 shows an annular venturi developed by the C.E.G.B. (P3) for measuring coal/air flow rates. The original concept was proposed by Graczyk (P3) who had previously conducted a set of tests, and it seemed that particle size was not very important as long as there was a reasonable distribution of particle sizes in the stream. The venturi required calibrating, which introduced measuring problems if it were to be used on an existing installation, and the pressure tappings gave unreliable readings, but a 10% error was the worst that was recorded. Its suitability with highly abrasive coals is open to question.

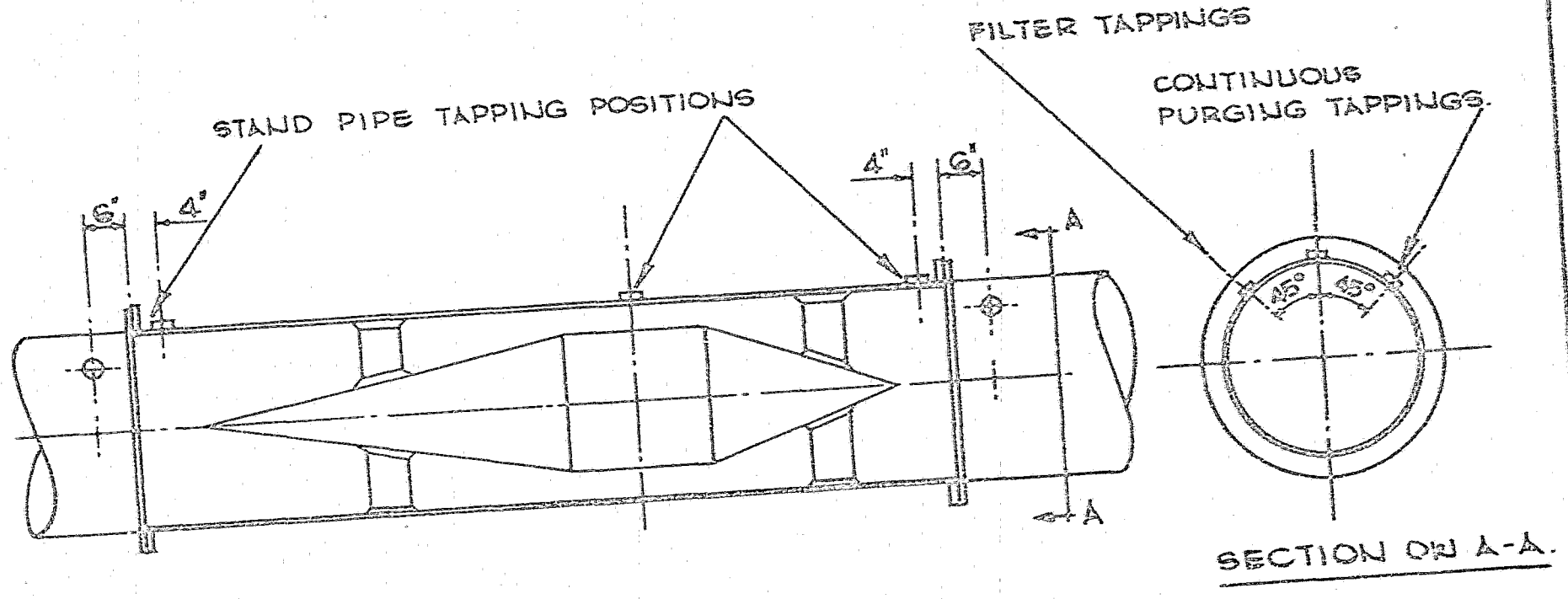

FIGURE 3,14: Annular venturi (from P3)

A more elaborate method of mass flow measurement was employed by B.C.U.R.A. (P11), whereby the absorption of β -particles by the coal dust was measured as a function of its concentration. By combining this with the velocity of the air (measured ultrasonically), the mass flow rate could be calculated.

A theoretical assessment established the following particle terminal velocity ratios as a function of gas velocity:

Particle Size		V_t / V_f
96%	minus 75 μm	0.992
60%	minus 75 μm	0.978

The impression given was that this method was completely unsuited to industrial application.

A further investigation (P11) of on-line particle measurement utilised a piezoelectric crystal, which when inserted into the dust stream, and with it output suitably damped, gave a signal corresponding to oversize particle momentum within the dust stream. The crystal was calibrated by dropping glass balls on to it from a known height, and plotting response against particle momentum.

3.6 SIZE REDUCTION

Comminution has been studied in great detail in the last 2 or 3 decades, since the economic factor has become all the more important, and processes have become more efficient and intense. Various theories have been postulated and tested, and for each theory put forward, there has been some practical evidence to fit certain conditions,

but no universal theory has, to the writer's knowledge, been formulated. In any event, the more accurate the theoretical approach, the more involved the laboratory testing becomes to determine the necessary constants and factors for a specific material.

3.6.1 Kick's, Rittinger's and Bond's Laws

A controversy has existed for a century as to the validity and applicability of Rittinger's and Kick's Laws applied to grinding.

Briefly, the energy equation (Walker, G1)

$$dW/dx = -K_2/_xN$$

has been used by various authors. For $N = 1$,

$$W \propto \log x_1/x_2 \qquad \text{(Kick's Law)}$$

and for $N = 2$,

$$W \propto (1/x_2 - 1/x_1)$$

or

$$W \propto (S_2 - S_1) \qquad \text{(Rittinger's Law)}$$

Here subscript (1) refers to the feed, and (2) to the product. That is, Kick stated that energy varies as the volume or mass change, and Rittinger stated that energy was proportional to surface area increase in a comminution process. "Any direct relationships between surface energy increase and energy requirements for fracture have been shown experimentally to be erroneous" (G24).

Bond (G5) proposed his Third Law of Comminution which results from putting N = 3/2 :

$$W \propto (x_2^{-\frac{1}{2}} - x_1^{-\frac{1}{2}})$$

A Work Index W_i was introduced to define the spectrum of breakage size, ranging from ∞ to x_2 = 80% minus 100 μm:

$$W_i = W \left(\frac{\sqrt{x_1}}{\sqrt{x_1} - \sqrt{x_2}}\right) \sqrt{\frac{x_2}{100}}$$

When W_i is known, the energy input W to effect breakage from size x_1 to x_2 can be calculated. This meas that W_i has to be determined by a laboratory or pilot plant test. As Arbiter et al point out, the integration of the above equation for N = 3/2 appears doubtful, because W_i, the proportionally constant, is a function of x.

3.6.2 Further Relationships

A study of grinding kinetics by Arbiter and Bhrany (G1) led to the equation:

$$D(x) = K_o \, t \, (x/x_o)^{\alpha}$$

This equation was derived from experimentally observed results which indicated that the rates of formation of finer sizes were substantially constant, and also that there was a dependence of initial grinding rate on screen size raised to a power α . The above equation has been shown to be experiementally correct for fine sizes and short grinding times, which makes it of practical interest in most grinding applications.

A breakage function of the form

$$F\ (f,\ x) = \frac{1 - e^{-x/f}}{1 - e^{-1}}$$

where f refers to feed size, and x to product size, was suggested by Broadbent and Callcott (G8), and was applied by Greenwood (G19) to the results of individual and collective breakage of particle assemblies. The resulting matrix showed two breakage mechanisms: one where the product size distribution showed a common relation when plotted against x, and the other a common straight line relation with x/f, the feed size being larger in the first case. To enable the breakage to be followed closely and accurately, the coal particles were labelled radioactively using tritium gas. This method gave a uniform distribution of radioactivity throughout the cross section of particles of up to 12 mm diameter, but could only be used for porous type material. Studies using neutron irradiation of coal have also been made by Gardner and Austin (G19).

Beke (M2) published a treatise on comminution, many of his findings being based on extensive ball mill tests carried out on various materials over varied residence times. A fourth theory was therein presented, this being the Walker equation modified and combined with the Schuhmann equation. By combining this with the Rosin-Rammler correlations and by referring to a logarithmic argument of the particle size distribution, the energy equation was derived:

$$W = K_3 \left[\frac{n_2\sqrt{1.781}}{x_{O_2}} - \frac{n_1\sqrt{1.781}}{x_{O_1}} \right]$$

CHAPTER 4

DESIGN AND THEORETICAL ANALYSES OF MILL OPERATING PRINCIPLES

4.0 INTRODUCTION

Mill manufacturers today have available a comprehensive range of mill sizes for industrial use, and when design is mentioned, it implies in essence selection of the correct type of mill to perform satisfactorily the duty specified. Although coal will be implied as the material to be ground in the following discussion, for industrial grinding of clays, bentonites, limestone, etc., a knowledge of the parameters listed below is required.

4.1 MILL SELECTION

The mill designer will have available curves of mill performance showing throughput as a function of:

Hardgrove Index,
Fineness,
Roller wear,
Power consumption, and
Feed size.

Normally a basic mill throughput at fixed fineness, Hardgrove Index, and feed moisture is specified and correction factors are used to calculate any other condition.

Comparative curves for various mills are given in the Appendix. It will be seen that the manufacturers have differing views on how certain conditions affect mill performance, although all trends are in agreement.

Besides the basic mill data a knowledge of various properties is required, these being:

- Feed size
- Product size - usually two mesh sizes
- Feed moisture - surface and inherent
- Product moisture
- Feed Abrasive Index and Hardgrove Index
- Temperature limitations on the material
- Material temperature at feed.

The system data required is:

- Material flow rate, t/h
- Temperature and pressure of hot air or gas available for mill drying
- Temperature and pressure of the air/fuel mixture required at the burner
- Barometric pressure, humidity and ambient air temperature limits.

4.1.1 Coal Throughput

By calculating the moisture content of the coal and knowing the feed and product fineness, the throughput can be calculated using the appropriate correction factors. It is as well to note that for roller mills there is a fall in grinding efficiency (and hence throughput) with roller wear so that for the purpose

of guaranteeing performance this should be taken account of by oversizing the throughput requirements. For control purposes a throughput margin is also required so that when operating an automatic control a fluctuating load swing will not temporarily overload the mill.

4.1.2 Product Size

The pulverised fuel burners used in modern power stations incorporate swirl vanes of various geometries to impart mixing to the air/fuel mixture, and use secondary and tertiary air supplies for efficient and complete combustion. However, the most important aspect of efficient burnout is correct particle size at the burner, i.e. from the mill. The standard practice ranges from 90 to 96% of minus 100 mesh, i.e. 65 to 75% of minus 200 mesh. Other sieve sizes can be obtained from a plot of the Rosin-Rammler equation.

It is important that the mill has a classification circuit which is capable of an efficient size cut of the mill circulating load. Both rotary basket, whizzer, and static types of separator have proved successful for such a product sizing. Roller mills have separators incorporated above the grinding chamber as an integral part of the mill which reduces space requirements as compared to the siting of an external separator above the mill (as for a tube mill).

The method of oversize fines return from a separator is important from the entrainment point of view, and the proper design of tailings flaps in the inner cone of the static type will prevent air by-passing the separator vanes, thereby lowering the efficiency.

If power considerations are important, this must be borne in mind with the rotary type where an approximate figure would be 0.4 kW/t milled, depending of course on the material's relative density and product fineness.

4.1.3 Air Requirements

It is common boiler practice to utilise waste heat in the boiler outlet gas to heat mill primary air for coal drying and promote stable combustion, as well as to improve the overall plant efficiency. Very often the coal moisture is so high that the hot air requirements for drying far out-strip the normal conveying requirements within the mill. When this high moisture condition occurs, the air/fuel ratio will be high and hence velocities will be higher than normal within the mill. Normally an upper surface moisture limit is set at 15% with a pulverised fuel surface moisture of 1 to 2%. Mill outlet temperature should be maintained above 80°C for the best combustion results. Mill inlet temperatures on boiler plant will not usually exceed 300°C unless an auxiliary air heater is used solely for mill air.

If moisture is low, the minimum air required is governed by mill and louvre velocities such that the coal is conveyed to the separator and out of the mill without chokage. Louvre velocity must be high enough to prevent spillage into the reject boxes, but at the same time to allow genuine reject material of higher relative density to fall through.

The heat required to dry the moist coal must come from the heated primary air, and this will be the dominant factor in sizing the P.A. fan, as well as the overall system resistance imposed on the fan.

The particle size-range transported to the separator from the table spillage will depend on the shape and velocity of the annular air stream. In general, the oversize material should be allowed to settle back on to the table before entering the separator, so as not to overload it and create too high a recirculating load within the mill body. In this connection, the wear rates will be adversely affected by high velocities and recirculating material.

Pressure drops are difficult to calculate for the loaded mill conditions and are normally related to existing installations, bearing in mind material relative density differences. However, a correctly designed annular louvre ring will lower the mill differential appreciably as this is where the highest pressure drop occurs.

4.1.4 Grinding Media

The table rotational speed is fixed for a particular mill in the majority of cases, unless the mill is belt-driven and the speed can be easily changed. The table speed influences the grinding efficiency of the rolls by varying the amount of the feed it presents under them, and by causing adequate spillage over the dam ring into the annular air stream. The speeds are derived from operating information, and are normally higher for sticky materials, although no fixed rules exist for the amount of speed increase.

Allied to the table speed is the roll size. The roll axis does not pass through the table vertical and horizontal suface axis intersection point, but above it, resulting in a slipping action between table and

roll, which is important in the grinding process as it promotes the wedging action of the material between roll and table. It may be necessary when grinding certain materials which tend to pack on the table to put ridges in the table and rolls to keep the material loose, and thus grind, not on a soft bed, but on the hard table segments. This packing action is fairly common with high moisture materials.

To cope with the slipping action between roll and table which promotes wear of both items (see Figure 4.6, which shows a worn roller and table), the wear increasing at disproportionately high rates with abrasive materials, special cast steel alloys are used for rolls and table, the most popular being Nihard.

4.1.5 Mill Power Requirements

Due to the nature of rock formation, which differs around the world, no two coals can with certainty be said to be alike from a comminution point of view. The Hardgrove Index attempts to interrelate various coals, but it is often only a guideline to actual operating conditions as will be explained in detail later. If operating data is available for a particular coal, this is the best guide for accurate power consumption. The comminution process is not steady powerwise, but gives rise to a fluctuating load of 15% or more which the mill motor must be capable of handling without tripping out. Power consumption for a South African Power station coal (Hardgrove 56) averages around 8 to 9 kW/t when grinding to 95% minus 100 mesh in a roller mill.

The mill motor is usually designed for start-up torque to be 225 - 250% of full load torque, as shown in Figure 4.1. This torque results from a stalled or crash shut-down condition where there is coal on the table at start-up. On larger mills - in particular the Loesche LM25 two-roll and the LM32 four-roll mills - the rolls are hydraulically lifted off the table at start-up to obviate this problem. The fairly high inertia of the cast table and gearbox components nevertheless helps to smooth out the high fluctuating load peaks.

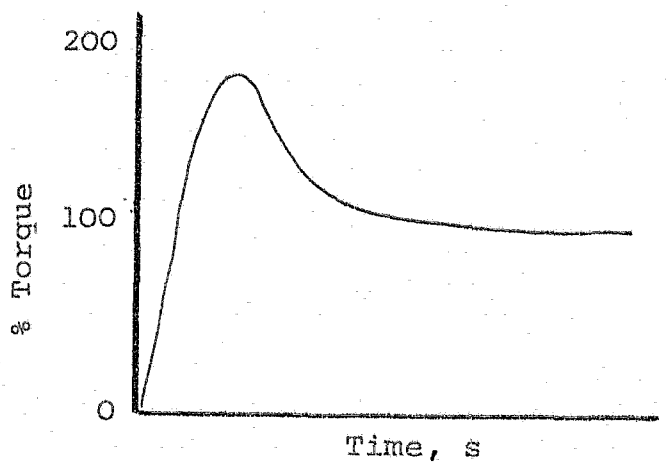

FIGURE 4.1: Typical starting torque on load

4.1.6 Air Flow and Temperature Regulation

Heated air is supplied from the forced draught under pressure to the P.A. bus-main, from which each mill P.A. fan draws off regulated amounts of hot air. Various designs of venturi meter the air flow, and

the temperature is recorded by means of thermocouples. The hot air enters the mill and dries the wet coal feed, leaving the mill at a preset temperature, usually between 80 and 95°C. If a dry batch of coal is fed into the mill, the mill outlet temperature will rise, but this will automatically be checked by drawing in cooling air with the hot P.A. at the P.A. fan inlet. Conversely, if the coal is too wet and the mill outlet temperature drops, the cooling air damper will close, and the feed is reduced, or the air through the mill is increased.

P.A. volume is adjusted by either a fluid-coupled or inlet vane-controlled fan. Normal practice is to control 70 - 100% air mass of rated fan capacity for 30 - 100% of mill throughput capacity (see Figure 4.2).

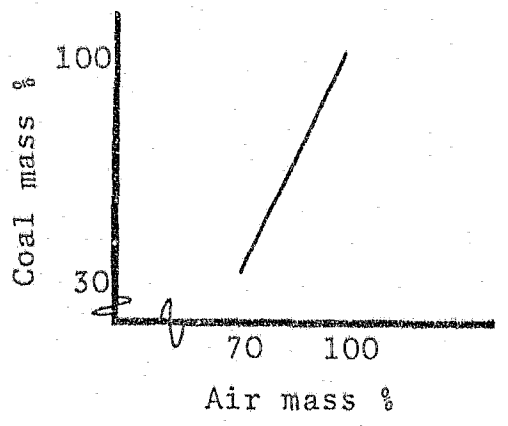

FIGURE 4.2: Air/Coal Control Curve

The volume of air passing through the mill for a given load will affect the fineness and load capacity of the mill as well as the final mill outlet temperature. As mentioned previously, the drying requirements often size

the P.A. fan, but there is a minimum velocity for pipe conveying and a maximum dust-air concentration which must be adhered to for safe operation. This has often been expressed as

$$v = 30/(A/F)$$

where v is the pipe conveying velocity in m/s, and A/F is the air/fuel ratio.

High velocities give poor fineness and increased mill wear, whereas low velocities will result in high reject rates, lower throughput, and increased fineness but also increased risk of mill chokage.

4.1.7 Throat Width

The coal spillage from the rotating mill table contains a considerable amount of oversize material which must be returned for further grinding. The shape of the air path, and the velocity of the air around the table, i.e. through the throat, are important aspects in efficient grinding. It is not possible to establish without extensive tests exactly what material size distribution spills off the table, therefore size spectrum must be assumed to be a combination of the feed and product sizes and the throat size designed accordingly. Obviously a happy medium has to be struck for optimum conditions and this usually depends on the nature of the coal and fineness required. Adjustments to the throat width can usually be made by blanking off part of a port, and this gap is then left as a permanent fixture not adjustable during operation.

The condition where particles are merely suspended in a fluid bed within the mill is undesirable since this leads to a pressure drop without throughput, and also leads to high abrasive wear. The velocity must therefore always be kept high enough for transport of the particles to a velocity zone where they either fall back for further grinding, or are transported to the separator. At the same time, reject material of high relative density must be allowed to drop through the throat into the reject boxes. Since the reject material should have a relative density of at least twice that of coal (Messerschmidt, M24), the terminal velocity will be $\sqrt{2}$ times higher, or conversely, a particle 1.4 times smaller than the equivalent coal particle will have the same terminal velocity as the coal particle.

It is, therefore, apparent that a quantitative analysis of fluid bed behaviour is very difficult to produce. However, by referring to the Arnot milling tests, some indication of voidage can be reached. Obviously the voidage will not be lower than that for a bed of coal, i.e. approximately 0.5 to 0.6 (Leva (F5)) at minimum fluidization, but the lower the voidage the higher the pressure drop per unit height.

Consider a fluidized bed* with a superficial air velocity of v and a voidage ε. It follows that the interstitial velocity v_ε within the bed will be higher than the superficial velocity v because of a smaller flow path.

---

* A fuller discussion of fluidized bed techniques is given in Chapter 6.

$$\therefore v_\varepsilon = v/\varepsilon \quad \ldots\ldots\ldots\ldots\ldots\ldots\ldots\ldots\ldots\ldots (4.1)$$

i.e. as $v_\varepsilon \rightarrow v$, $\varepsilon \rightarrow 1$. Clearly for a stable flow condition,

$$v_\varepsilon = v_t$$

where v_t is the terminal velocity for a bed of particles.

From Figure 6.22 the following experimental trend holds:

$$- m \log \left(\frac{1-\varepsilon}{\varepsilon^3}\right) = \log v \quad \ldots\ldots\ldots\ldots\ldots\ldots (4.2)$$

where m is the slope of the gas-solid expansion curve. Similarly, m is dependant on particle diameter d (Figure 6.6):

$$m = F(d) \quad \ldots\ldots\ldots\ldots\ldots\ldots\ldots\ldots\ldots\ldots (4.3)$$

Substituting (4.3) in (4.2),

$$\log v = - F(d) \log \frac{1-\varepsilon}{\varepsilon^3} \quad \ldots\ldots\ldots\ldots\ldots (4.4)$$

and from (4.1),

$$\log v_\varepsilon = - \log \varepsilon - F(d) \log \left(\frac{1-\varepsilon}{\varepsilon^3}\right) \quad \ldots\ldots\ldots (4.5)$$

That is, the bed terminal, or settling, velocity decreases with decrease in voidage for a given particle size, or the bed terminal velocity decreases with particle size for a given voidage.

If the particles in the bed are considered individually then the particle drag is given by:

$$F_D = \frac{1}{2} C_D \rho_f A v_\varepsilon^2 \quad \ldots\ldots\ldots\ldots\ldots\ldots\ldots\ldots \quad (4.6)$$

whence the terminal velocity for a particle falling under gravity is

$$v_\varepsilon = \sqrt{\frac{4 (\rho_s - \rho_f) g d}{3 \rho_f C_D}} \quad \ldots\ldots\ldots\ldots\ldots\ldots \quad (4.7)$$

Substituting v/ε for v_ε in (4.6),

$$F_D = K_4 v^2/\varepsilon^2 \quad \ldots\ldots\ldots\ldots\ldots\ldots\ldots\ldots \quad (4.8)$$

which for a given superficial velocity and particle size gives

$$F_D \propto 1/\varepsilon^2 \quad \ldots\ldots\ldots\ldots\ldots\ldots\ldots\ldots\ldots\ldots \quad (4.9)$$

for a single particle in a fluidized bed.

Also for the same superficial velocity v, from (4.1) and (4.7), and since $\rho_s \gg \rho_f$, $(\rho_s - \rho_f) \approx \rho_s$

$$\therefore \frac{v_{\varepsilon_1}}{v_{\varepsilon_2}} = \frac{\varepsilon_2}{\varepsilon_1} = K_5 \sqrt{\frac{\rho_{s_1} d_1}{\rho_{s_2} d_2}} \quad \ldots\ldots\ldots\ldots \quad (4.10)$$

that is, for $\varepsilon_1 = 0.8$, and $\varepsilon_2 = 0.4$, for suspension,

$$v_{\varepsilon_2} = 2 v_{\varepsilon_1}$$

and either $\rho_{s_1} = 4 \rho_{s_2}$ for the same diameter, or
$d_2 = 4 d_1$ for the same density.

Assuming that the particle size remains constant (i.e. table spillage does not vary), then the higher density material will be suspended above the throat. Since this region is turbulent, it can be expected that the high density material will migrate to the bottom of the bed and eventually reach the throat area where the velocity v is too low to suspend it, whereupon it falls through the throat as reject material. The advantage, therefore, of operating at low voidage above the throat is that the terminal velocity difference v_{ε_2} (at $\varepsilon = 0.4$, say) to the throat velocity v (which is higher than the terminal velocity for the largest single coal particle (i.e. one of low density)) is large and there is therefore the greatest probability of high density material rejection.

The throat design should therefore incorporate the following features:

(i) The throat velocity must be higher than the terminal velocity of the largest single coal particle spilling off the table. (In practice this is considerably smaller than that of the largest feed size and as an approximation may be taken as 25% of feed size).

(ii) The fluidized bed region must contain all material so that a low voidage can be maintained.

(iii) The fluidized bed must not extend into the throat area - this will cause high wear and pressure drop.

(iv) The system resistance will be higher for the low voidage and due allowance must be made for this when sizing the system fan.

(v) If the total air requirement for the mill exceeds the throat mass flow required, then the air flow may be split to introduce air above the throat as well as through the throat. This will enable the throat velocity (and therefore width) to be adjusted to give optimum voidage.

There is also reason to believe from fluid bed heat transfer tests that the lower voidages give higher heat transfer coefficients. Since the coal spilling off the table is still moist, the main drying area is above the throat (the P.A. being normally at 230°C to 270°C) and a higher drying efficiency will result in a drier recirculated product on the table and hence better grinding when this recycled dry material mixes with the new wet feed.

4.2 MILL OPERATION AND OPERATING PARAMETERS

Some of the operating features and control parameters of a roller mill are given below.

4.2.1 P.A. Differential Pressure (abbreviated 'P.A. diff')

The P.A. diff is the pressure measured at the P.A. flow orifice or venturi, and is calibrated against air flow

by a pitot traverse across the duct. It is used as the controlling signal for air supply to the mill, and is set on each mill according to the individual calibration curves.

4.2.2 Mill Differential Pressure (abbreviated 'mill diff')

The pressure drop across the mill from mill inlet to mill outlet is the mill diff. With increasing P.A. diff, the mill diff of an unloaded mill would vary linearly (curve (1) of Figure (4.3)). Curve (2) would then be the loaded condition - this would not necessarily be linear.

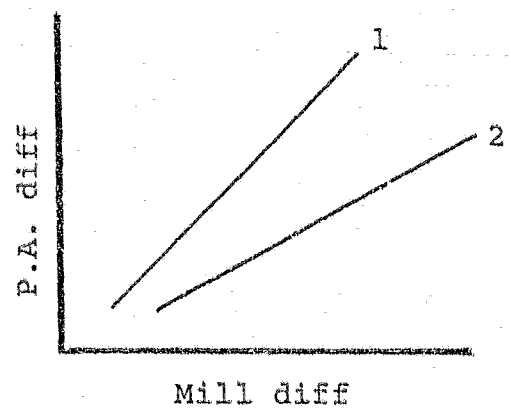

FIGURE 4.3: P.A. diff - mill diff curves

The mill diff is an indication of the amount of coal in the mill (and therefore of the throughput under steady conditions) and it is thus used as the pri: ary control signal. If the mill diff increases, the mill resistance across the mill has increased and the P.A. volume therefore drops. The P.A. flow is controlled either manually or by a boiler master signal, and this in turn controls the

mill diff via a preset calibration on-load curve. The mill diff in turn controls the feeder. Thus if chokage were to occur, the mill diff would increase, decreasing in turn the P.A. diff. The P.A. would pick up the boiler master signal, and the mill diff would control the feeder by decreasing the feed rate until the chokage had cleared.

4.2.3 Air/Fuel Ratio

The on-load curve is set by calibration tests during commissioning, and, in effect, governs the air/fuel ratio throughout the operating range of the mill. The burner characteristics determine what air/fuel ratio is suitable to maintain stable combustion. At full load, air/fuel ratios of 1.5 to 1.7 are normally used, and these go up to 3 for partial load conditions. Lower A/F ratios result in a high mill diff and consequently a higher pressure fan (see Figure 4.4).

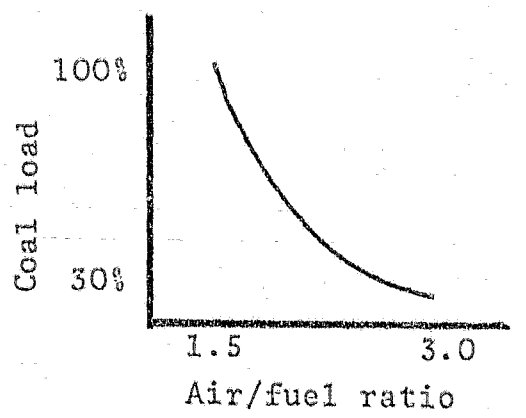

FIGURE 4.4: Air/Fuel ratio vs throughput curve

4.2.4 Separator Settings

Whizzer type

The whizzer separator speed is controlled from the mill

control panel by increasing or decreasing the speed of the variable speed motor or gearbox drive. Speeds in the range 60 - 120 r/min are normally used for coal mills. Increasing the speed will increase the fineness of the product by increasing the recirculating load within the mill, i.e. returning a higher mass of material to the table for regrinding. This will result in a higher mill diff and thus a reduced load.

Whizzer operating features to consider are:

- Ease of adjustment during operation
- High running cost
- High initial cost
- High blade wear
- Sealing problems on bearings
- Re-entrainment of oversize particles

Static Vane Type

This separator has no moving parts and is preferred for grinding applications for which conditions are steady. The vanes are adjusted and set during commissioning to the optimum angle, and are manually adjustable - normally one at a time. The greater the angle between vane and radius the finer the product.

Features of this sytem are:

- No maintenance
- Low initial cost
- Oversize returned directly to the table via flaps in the inner cone

- More difficult to adjust
- Not suitable on variable process requirements
- Slightly higher pressure drop

4.2.5 Roll Pressure

The rolls are adjusted with a slight gap between the table and roll so as to avoid damaging the cast table segments when running the mill empty. The roll pressure is adjusted either by compressing the springs (as is done at the Camden Power Station) or by changing the hydraulic roll loading pressure, the latter being easily achieved during mill operation.

With new rolls, i.e. before wear has occurred, the gap between table and roll is between 6 and 37 mm (Figure 4.5) and the pressure exerted to grind coal is a function of this gap. As the rolls wear, this gap increases, and to maintain the same grinding pressure on the table, the roll pressure should be increased. This will help to maintain the required fineness and keep the reject rate low. However, higher roll pressure will also increase the absorbed power by imposing a higher rolling resistance, and the optimum setting has to be found for each type of product being ground. Since the slippage between the table and rolls is the cause of the wear of the rolls, for high roll pressures, the scouring action of the coal will be more severe, resulting in lower roll life. Here again, optimum settings are found by examining wear patterns for various roll pressures over a number of months to get the longest life out of the rolls. Figures 4.6 and 4.7 show various aspects of roll wear.

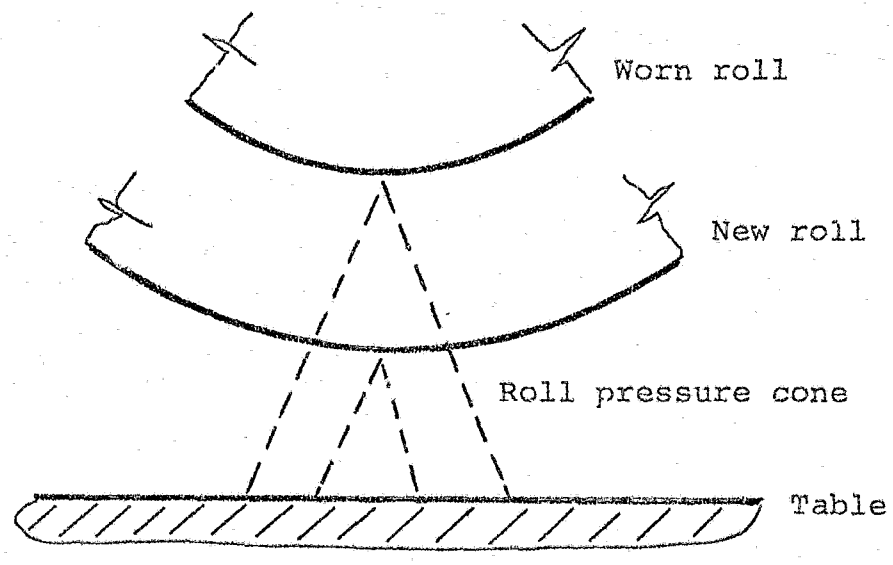

Figure 4.5: Roll pressure conditions

4.2.6 Dam Ring

The ring retaining the coal bed on the table - the dam ring (see Figure 4.6) - governs the amount of spillage, size of material ground and bed thickness. It is therefore important to optimise the height of the dam ring during commissioning, after which it should not require changing. A low dam ring will give thin bed grinding and lower power, but more spillage of over-size material into the louvre air stream. This results in a coarser product, since coal on the table is not retained long enough to undergo the necessary grinding action.

The dam ring must always be sized at the operating roll pressure since the wave of coal in front of the roll spills over the dam ring (Figure 4.8). Obviously, the higher the roll pressure, the higher the wave resulting in the need for a higher dam ring if spillage is too great.

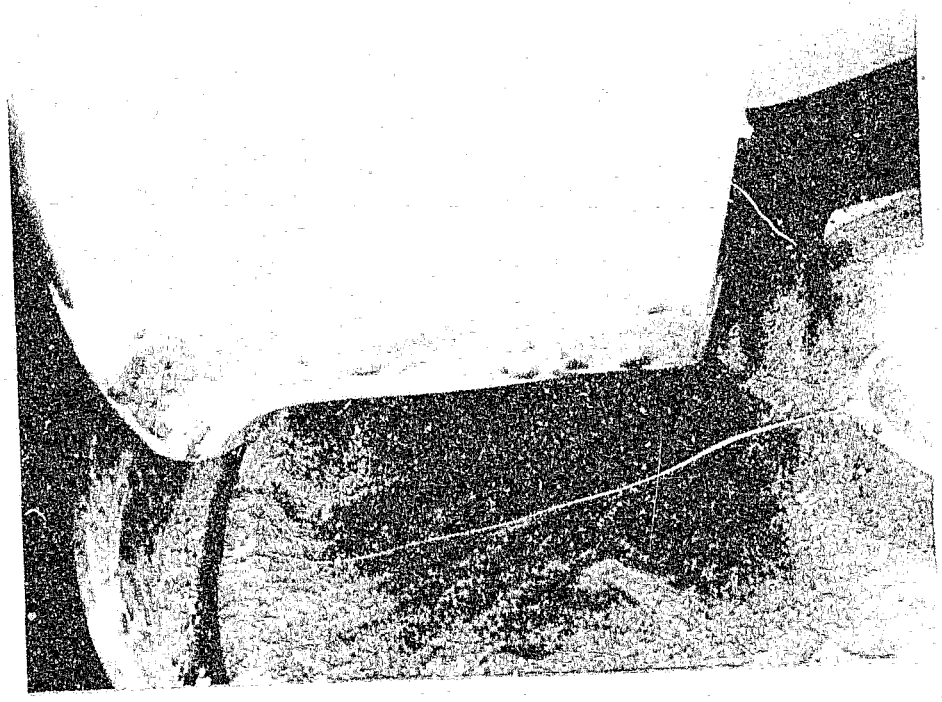

FIGURE 4.6: Roll and table wear-dam ring at lower left (from Arnot tests)

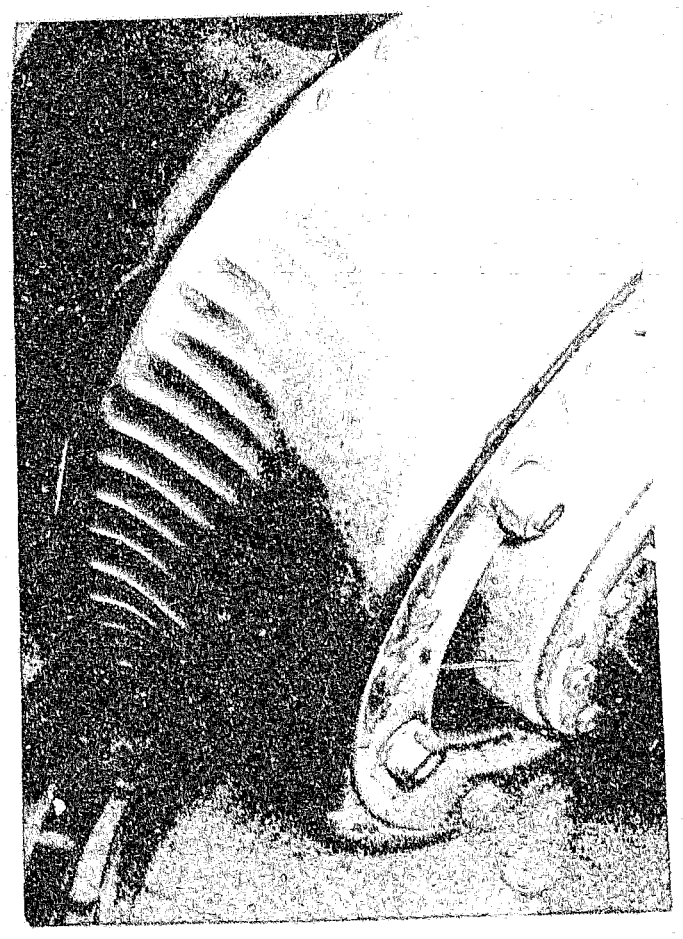

FIGURE 4.7: Roll ridge pattern (from Arnot tests)

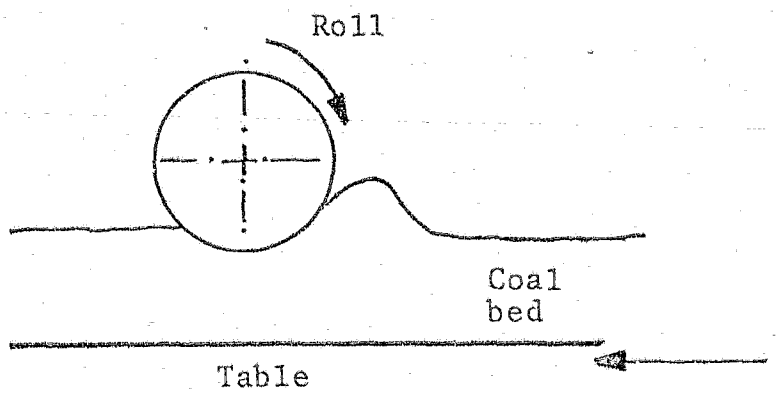

FIGURE 4.8: Coal wave ahead of roll

4.2.7 Reject Adjustment

The bulk density of raw coal feed is approximately 800 kg/m^3, and for pulverised coal, 1450 kg/m^3. Anything in the coal with a relative density of over approximately 1.9 should be rejected as it is non-combustible material, usually with high abrasive properties.

The main parameters affecting rejection have been explained in the above paragraphs. They are:

- P.A. diff - the higher the P.A. diff, i.e. velocity through the throat, the less the reject rate.
- Coal size and material properties.
- Dam ring height. (If the spillage into the air stream is excessive, the reject rate will be high).
- Roll wear - which results in inefficient grinding and more spillage.
- Louvre throat width - which affects velocity.
- Roll pressure.

The total amount of material rejected is often dictated by economics, especially with the high pyrites content from run-of-mine coal with thin seams, but under normal circumstances even the rejected material usually represents only a small percentage of the total reject material in the mill feed. The optimum settings are therefore determined on this basis, and for normal operation on coal result in up to approximately 400 kg/h of reject material per mill (for manual reject removal). A float and sink determination with a fluid of 1.7 to 1.9 relative density will give approximately 10% or less sinks for a clean coal.

4.3 CONCLUSION

It will be noted that there are many influencing factors affecting the final operating condition of a mill, and that these effects are interrelated in most cases. During commissioning of a mill, the optimum performance has to be obtained and graphical correlations plotted. In the Appendix some graphs of actual test results are given with a suggested method of correlation.

CHAPTER 5

MILL MODEL TESTS

5.0 SCOPE OF TESTS

To study flow areas within a Lopulco mill, a model testing programme was embarked upon with the following aims:

- To study the flow phenomena by photographing, measuring and visually observing events in the model using appropriate scale-down factors and similiarity effects.
- To localise problems which should be studied in further detail.
- To become familiar with the aerodynamic working principles of a mill.

5.1 PHYSICAL FACTORS

The parameters to be considered for similarity purposes depend on what modelling basis, i.e. Reynolds or Froude, is to be used.

The mill measurable conditions are:

Air flow: air enters the mill at 230°C and cools to approximately 100°C within 1 m of the entrance point (i.e. the throat). The density variation is therefore

1.35 to 1, hence the velocity within the mill will vary as the air cools. This will obviously affect air flow patterns and is difficult to simulate unless a distorted model and/or heat sink is used.

Coal flow: the quantity of coal feed to the mill can be scaled down although size distribution is difficult to predict. Unless the model is actually grinding the feed material, the feed must be sized for practical conditions of flow within the model. This also applies to the pulverised fuel which is of unknown size distribution within the mill.

Separator speed: this speed can be scaled down to give a similar effect but because of the particle size distribution within a model, as explained above, the separator can be of little or no benefit in a flow model.

Table rotation: the table speed affects coal flow from the table into the air stream, but does not influence the air flow pattern significantly within the mill. It can therefore be ignored for modelling purposes.

5.2 FLOW VISUALISATION

During modelling, techniquies are often required to enable one to observe or measure physical effects in either gas or liquid flows, without resulting in disturbance to those effects by the measuring devices. These methods can also very often be applied to full scale prototypes (as in the use of radioactive tracers), but the present work concerns models only. If boundary conditions are known precisely and provided they are not too complex, a mathematical model will often describe the flow, and a complete solution can be

obtained using integration methods on a computer. Alternatively, by probing the flow field, and measuring its physical properties, an image of the whole field can be formed, e.g. by using Teledeltos paper or a pitot tube. (If Teledeltos paper is used, the flow must be assumed to be potential in character).

A quicker way is to photograph the flow. This doubles as a record of the patterns which might be constantly changing, and also, there are no disturbing influences on the flow: the photograph can thus be used both quantitively and qualitatively. The nature of the flow also determines the type of photography employed; a changing pattern would be best recorded on a cine film whereas a stable flow could be photographed using an ordinary still camera.

The model studies undertaken involved the use of water, one of the principal advantages of water being the relatively small size to which the model can be scaled. Various types of flow visualisation techniques were tried out, and although similarity had to be sacrificed to a certain extent, a successful study of various phenomena was achieved. Certain methods of water flow visualisation are as follows:

(i) A technique for laminar flow developed by Standford University uses the effect of electrolysis: tiny hydrogen bubbles are generated when a pulsed d.c. current flows through a wire in the water, and these bubbles can be photographed and the velocities determined if one knows the pulse intervals. This method is suited to open flow.

(ii) Dyes or additive solutions give good results if the liquid is disposable, as dyes will provide flow patterns at low velocities, or indicate mixing patterns in turbulent flow. Coloured milk and alcohol, to correct for density, are often used, but the point of injection must be carefully chosen if the desired effect is to be clearly visible, especially for purposes of photography.

(iii) Boundary effects can be well observed by fixing cotton tufts onto the inner walls of the flow vessel, but these have the disadvantage that no real comparison can be made as to velocity gradients, since they take up the direction of flow over the whole velocity range. (Reverse flow phenomena and turbulence were two of the observed effects in a 1/6th scale model of the mill which used cotton tufts, and such flows were verified in a slice model as well).

(iv) Radioactive tracers have been widely used to trace flows and detect leaks - radioactivity is not affected by temperature and γ-ray emission can be detected through intervening materials. Radioactive liquid (labelled) has been floated on an unlabelled liquid and the velocity determined by the number of counts (Littlejohn and Spencer, (B7)).

5.3 MODEL DESIGN

In selecting the type of similarity to be used, the various forces within the mill must be considered. In this instance viscous forces were predominant and therefore Reynolds similarity was chosen. To enable the

model to be suitably sized for flow visualisation and measurement, water was used and a 1/6th scale model was selected.

For two-phase model studies the problem of similarity can be tackled in various ways; either sizes are similar, which leads to difficulties when the full scale material is itself small, or densities are similar, leading to impossible physical conditions. For the present study, since the full-scale material was in a size range from a few to a few thousand μm, and in the relative density range of 1.5 to 3, polystyrene beads were chosen with a relative density of 1.04. They could well be called a tracer as the density was so close to that of water as to enable them to follow the flow paths. The flow patterns of the beads in the mill model could be photographed, but only the boundary flow was clearly defined, and as the water went into a sump, the beads had to be removed in a wire mesh basket on leaving the model. Slit lighting through the model was attempted, but the bead concentration made it impossible to view the flow at the centre of the model.

A slice model of the mill therefore proved most useful for viewing the full flow through the mill in the two-dimensional plane. Since the flow velocity was very much higher than the rate of rise of the bubbles in water, there was no noticeable buoyancy effect when using the bubble technique described later.

5.4 3-DIMENSIONAL MILL MODEL TESTS

The model was a 1/6th scale moulded perspex model of the Lopulco LM14 pressure type mill with whizzer separator of the type installed at Camden Power Station. It was installed in a controlled flow system to assess the

effect of various design parameters and to enable the flow patterns within the mill to be measured.

The test rig comprised the following: a Sulzer 2 stage centrifugal pump rated at 2090 l/min at 70 m head driven by a 45 kW motor provided water which was regulated through a 100 mm pipe with a flow orifice to BSS installed in it and reading on a 1.27 m water over mercury manometer. A bypass pipe could also be used to return the water to the underground sump, and a non-return valve on the pump suction kept the pump full after priming (Figure 5.1).

The model was mounted on a 1.3 x 0.8 m diameter galvanised tank. To prevent bulging of the two ends of the tank, 6 mm thick mild steel discs were placed on the ends and connected with 6 mm tie rods. The water inlet to the tank was at the side at the bottom via a flanged joint. Since the water discharged from the model in an horizontal direction, an A-frame of "Handy Angle" was built around the model to secure it to the tank.

The water discharging from the mill was led via a 250 mm neoprene pipe into another galvanised tank of the same dimensions, which then drained into a 25 mesh steel basket 1.2 x 0.5 m in diameter via two 125 mm pipes. This basket was immersed in the sump, and collected the polystyrene beads used in the model.

A 50 mm suction pipe with a foot valve was immersed in the basket and connected to a Vacseal pump, which pumped the water/beads mixture via a 40 mm plastic hose to the feeder tank. This tank, 600 x 750 mm diameter, with a 480 mm conical lower end and enclosed top, was sus-

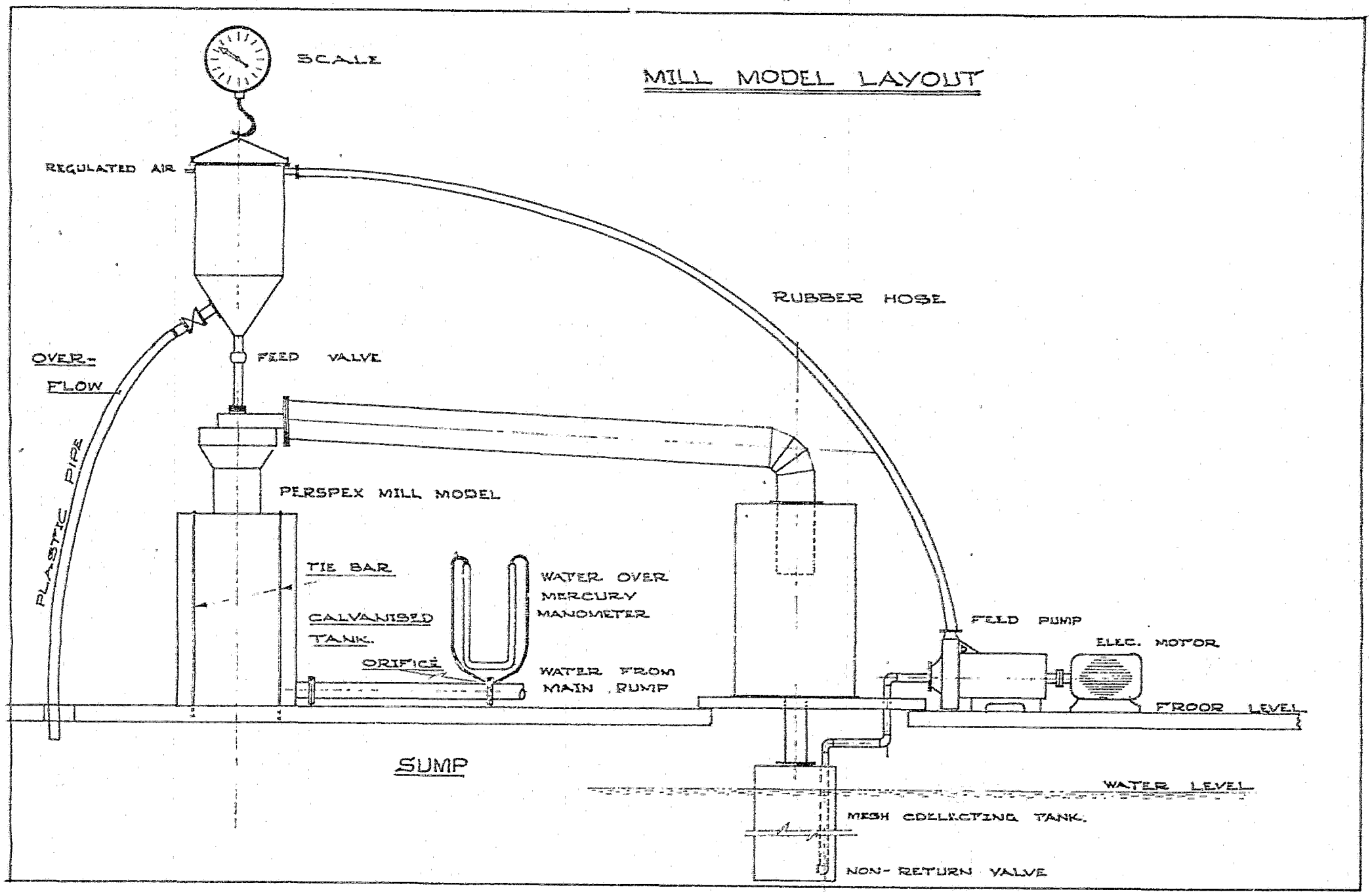

FIGURE 5.1: Mill model layout

pended on a 0-180kg Salter scale (reading in 0.45 kg divisions) above the model by means of a block and tackle. A slide valve and quick release coupling were connected onto the lower end of the conical section. Since the water/bead mixutre was very dilute, an over-flow pipe and valve with a 25 mesh screen on the inlet were installed to prevent beads from running out into the sump. An air connection onto the tank allowed the pressure to be maintained between 0 and 1.38 bar (which was considered a safe limit). Provision was also made for a water connection. The water/bead mixture was then pressure-discharged via the slide valve and 50 mm plastic pipe into the mill through the central chute. Figures 5.2 and 5.3 show the feed bin and a general view of the model arrangement, and calibration curves for orifice and feed bin are given in the Appendix.

Although the scale effect of the separator was considered of secondary importance, provision was made to rotate it at a scaled down speed. A capacitance motor adjusted by means of a Variac was mounted on the top of the model, and drove the separator through a reduction gear.

The model itself was moulded from 3 mm clear perspex with a detachable top for access to the inside. Roller inserts were machined and bolted to the stationary table, and the throat ring was made to resemble the original as closely as possible. For the purpose of accommodating the traversing gear, 3 mm holes were drilled in the sides of the model and plugged when not in use. Figures 5.4 to 5.8 show some of the model details.

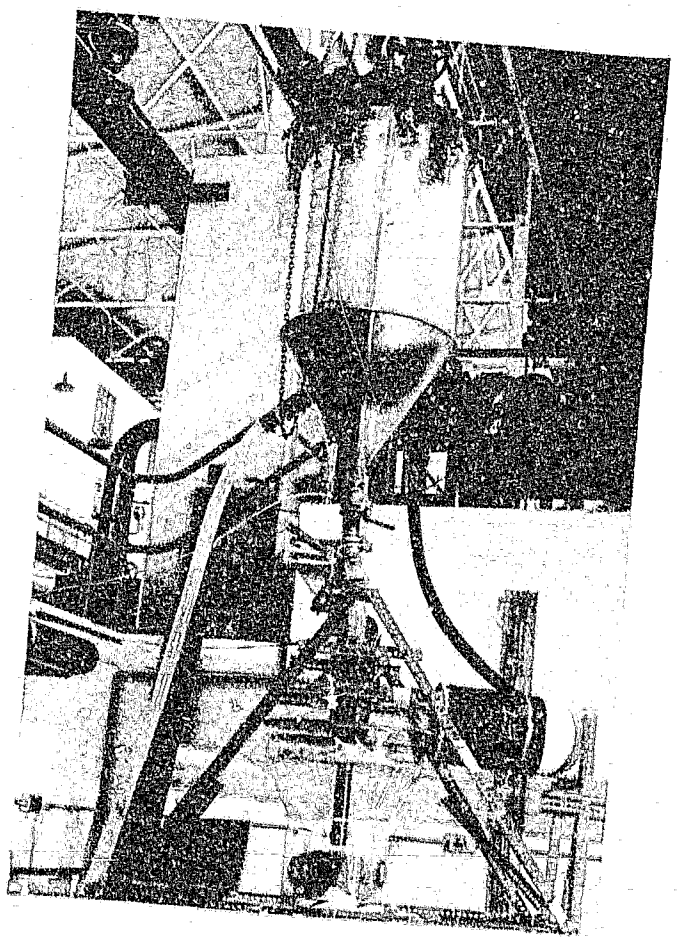

FIGURE 5.2: Feed bin and model

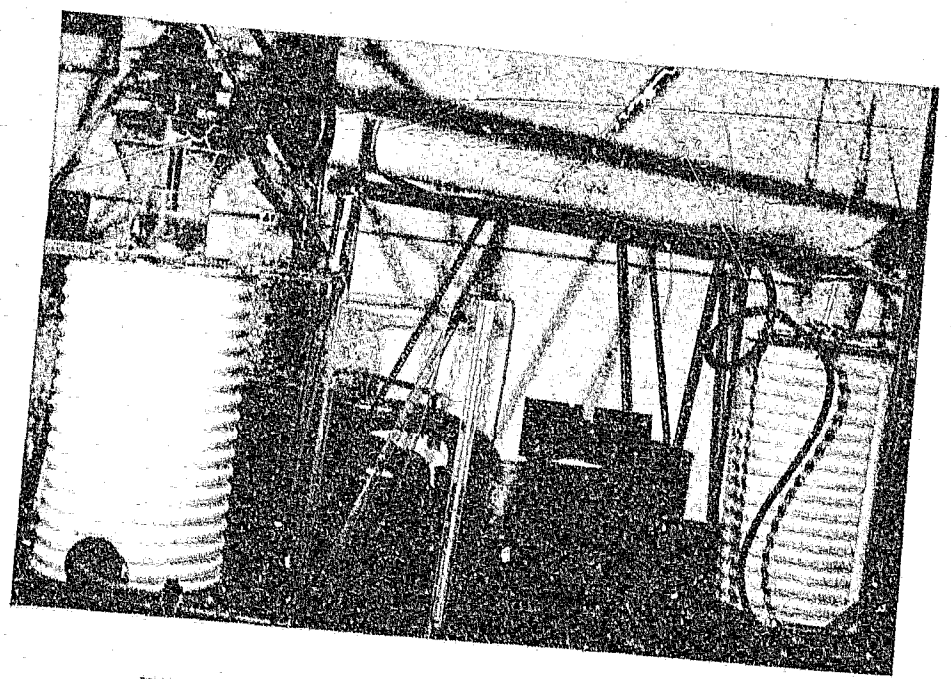

FIGURE 5.3: General view of model and discharge arrangement

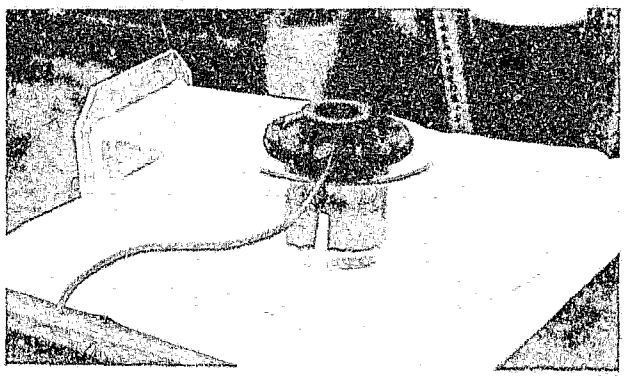

FIGURE 5.4: Mill top

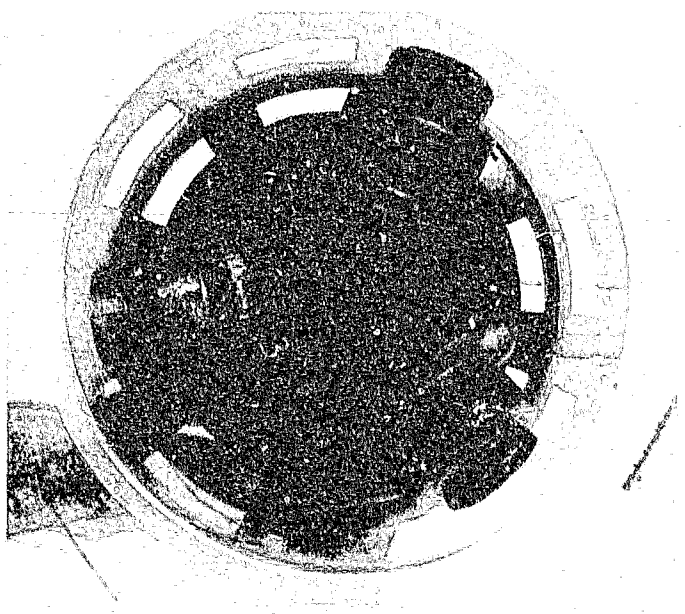

FIGURE 5.5: View into mill from top showing throat



FIGURE 5.6: Mill body

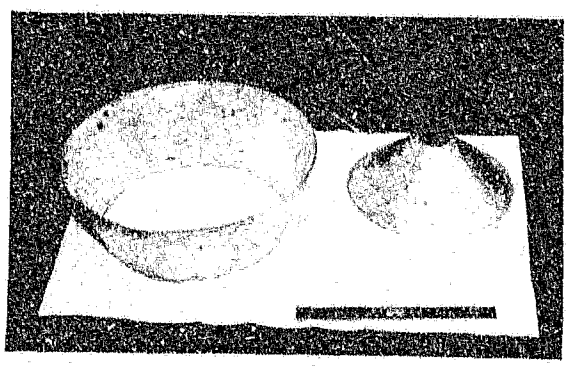

FIGURE 5.7: Cone inserts

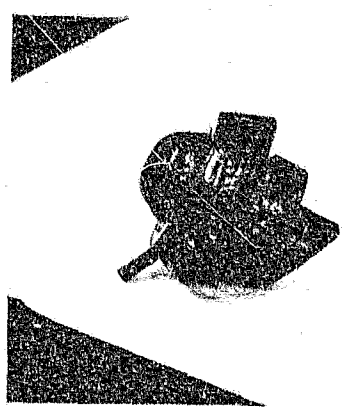

FIGURE 5.8. Roll insert

5.5 RESULTS OF 3-DIMENSIONAL MODEL TESTS

5.5.1 Flow Visualisation using Water and Beads (Figures 5.9, 5.10, 5.11)

The 'feed' was a mixture of water and polystyrene beads, diluted to allow enough fluidity when forced down the central feed chute under gravity and bin pressure. The beads flowed across the table and were picked up by the water flow through the throat, as shown in the photographs reproduced below. (The three rolls on the prototype each had a rather complicated cover protruding from the side of the mill for location of the roll axle and rocker arm, but this was omitted on the model as its effect was considered of secondary importance and it hampered viewing of the throat area).

As can be expected, the particle flow under the roll was small, but the turbulent pattern above it can be clearly seen in Figure 5.10 as well as the inclination of the flow imparted by the inclined throat. (In actual practice there is a wave of coal in front of each roll). The cotton stringers (Figure 5.11) clearly showed the flow direction in the mill's conical section, the angle of divergence of the sides to the vertical being 30°. This observation confirmed earlier predictions on the prototype of a recirculating load in this area. (Combined with oversize returning from the separator, this recirculation leads to high wear and pressure drop in the mill). The photographs also showed that there was considerable vorticity in the conical area - no doubt caused by the turbulence above the rolls.



FIGURE 5.9: Polystyrene beads - flow pattern between rolls

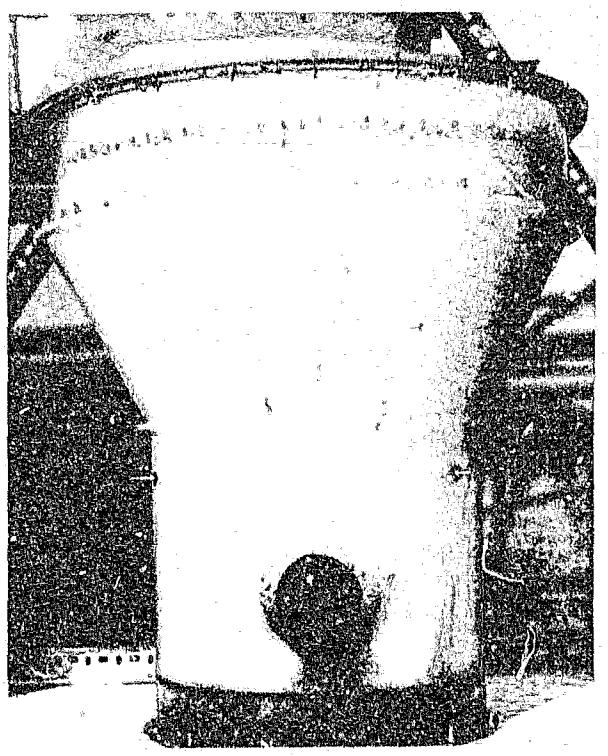

FIGURE 5.10: Polystyrene beads - flow pattern around roll

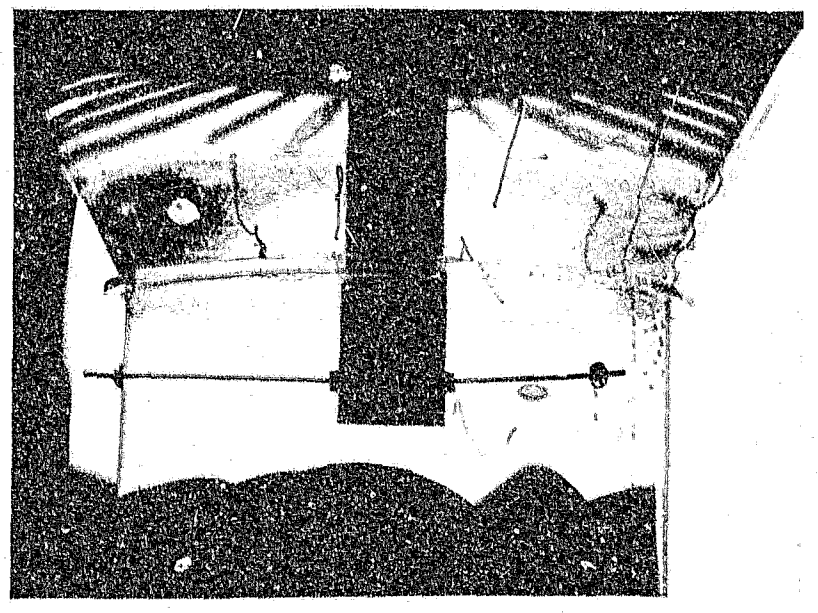

FIGURE 5.11: Reverse flow indicated by stringers

5.5.2 Pitot Traverse

Confirmation of irregular flow patterns on the water-body interface having been established visually, the next set of tests was aimed at establishing the flow pattern within the mill over the cross section. For this purpose, 3 mm holes were drilled up the side of the body in a position between two rolls. Because of the position of the rolls this was the only area that was accessible for the insertion of a pitot tube. A miniature pitot was used to determine velocity profiles across the mill radius by inserting it into these holes and traversing across the mill. Whilst traversing, the pitot was rotated to check the flow angle. However, the deviation from axial flow was negligible. The two plots seen in Figures 5.12 and 5.13 were made at different flows, but the general flow patterns were unchanged. (The lines of constant velocity are here shown in units of ft/s).

It is interesting to note that the areas of zero or reverse flow were as predicted by the first tests using stringers, and the flow breakaway can be clearly seen at the 30° body divergence. If the regions of zero velocity are defined by a linear boudnary, the angles subtended for Tests 1 and 2 are very similar. The flow rate for Test 1 was 55% of that for Test 2, thus covering the normal operating range of 70 - 100% air adjustment. The reverse flow effect region is enclosed by a boundary closely related to the nozzle expansion region.

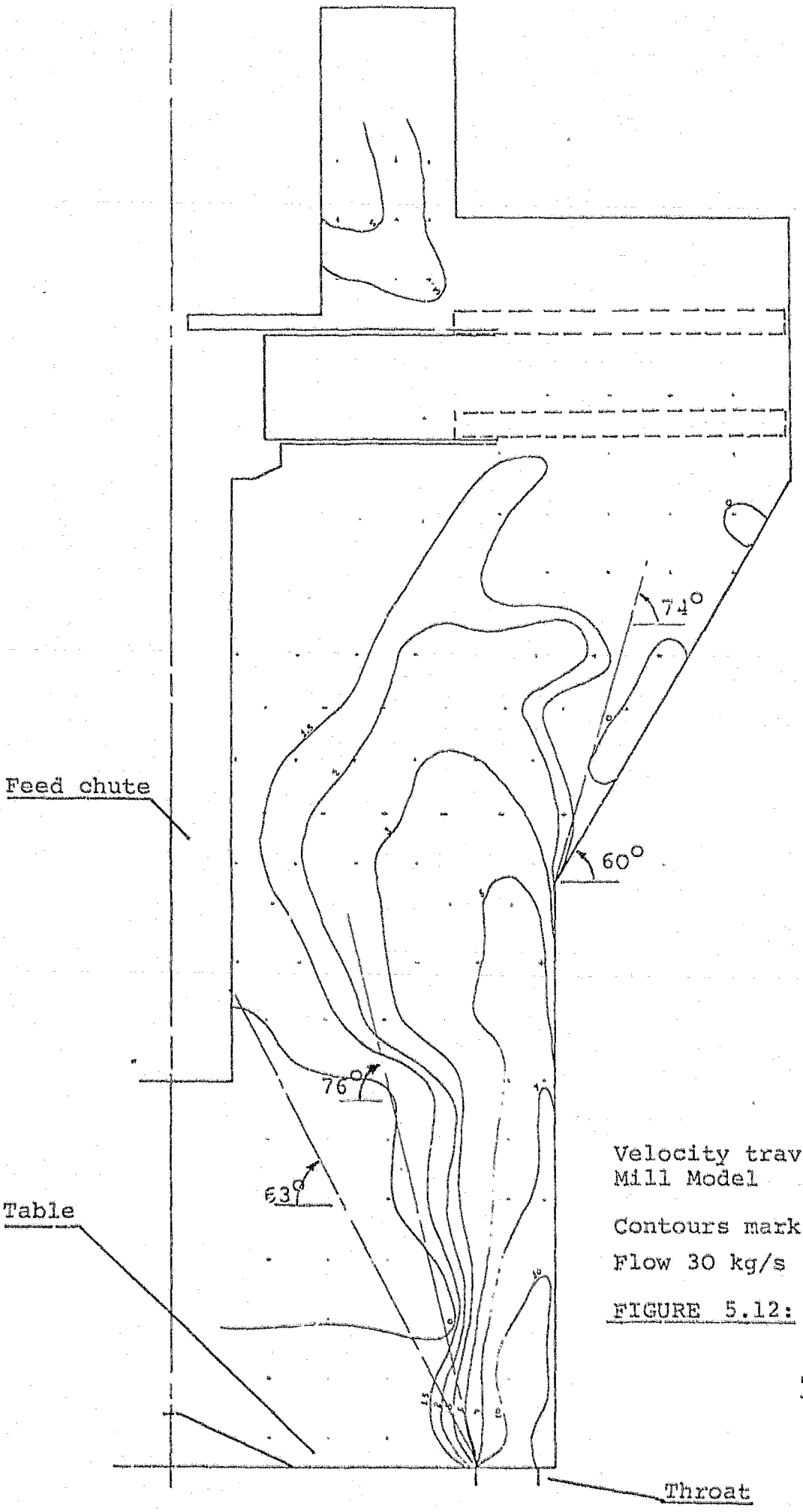

Velocity traverse of LM 14/3P Mill Model

Contours marked in ft/s

Flow 30 kg/s

FIGURE 5.12: Pitot traverse of model.

TEST 1

Author De Wet Kruger J I
Name of thesis A study of the parameters affecting the design of vertical spindle mills 1977

PUBLISHER:
University of the Witwatersrand, Johannesburg
©2013

LEGAL NOTICES:

Copyright Notice: All materials on the University of the Witwatersrand, Johannesburg Library website are protected by South African copyright law and may not be distributed, transmitted, displayed, or otherwise published in any format, without the prior written permission of the copyright owner.

Disclaimer and Terms of Use: Provided that you maintain all copyright and other notices contained therein, you may download material (one machine readable copy and one print copy per page) for your personal and/or educational non-commercial use only.

The University of the Witwatersrand, Johannesburg, is not responsible for any errors or omissions and excludes any and all liability for any errors in or omissions from the information on the Library website.